AN EXPERT SYSTEM FOR STRESS ANALYSIS OF HUMAN TEETH

By

Qiong Li

Dissertation

Submitted to the Faculty of the

Graduate School of Vanderbilt University

in partial fulfillment of the requirements for

the degree of

DOCTOR OF PHILOSOPHY

In

Mechanical Engineering

May, 2009

Nashville, Tennessee

Approved:

Professor Carol Rubin

Professor Prodyot Basu

Professor Roy Xu

Professor Samuel Mckenna

Professor Nilanjan Sarkar

Dedicated

to

Rachel and Peiyong

ACKNOWLEDGEMENTS

First and foremost, I would like to express my sincere gratitude to my advisor, Dr. Carol Rubin, for her guidance and help during my whole Ph.D. period. Appreciation also goes to other members of my dissertation committee, Dr. Nilanjan Sarkar, Dr. Prodyto K. Basu, Dr. Luoyu Roy Xu, and Dr. Samuel Mckenna for their comments and suggestions for this dissertation. I would like to express my appreciation to the Vanderbilt University Discovery Grant Program for funding this research through Grant 4-48-999-9116. Finally, I would like to express my gratitude to my family. Without their support and love, I would never have succeeded.

TABLE OF CONTENTS

Appendices

LIST OF TABLES

Page

LIST OF FIGURES

Page

CHAPTER I

INTRODUCTION

Subject and its Importance

Human dental structures, both natural and man-made, experience internal stresses which are of great interest to both practicing dentists and researchers. For example, stress resulting from regular chewing forces will not cause any damage to regular teeth, but once the teeth are damaged due to the loss of tooth tissue on a certain area, they are more sensitive to fracture due to stress concentrations in this area (Palamara et al., 2002; Topbasi et al., 2001). Restorations composed of various materials, thermal changes on restored teeth or the anomalous biting forces caused by hard food or anomalous chewing will also cause stress concentrations and make teeth more susceptible to fracture (Borcic et al., 2005; Ausiello et al., 2001; Toparli et al., 2003; Arola et al., 2001; Dejak et al., 2003; Toparli and Sasaki, 2003; Lin et al., 2006). The stress distributions on teeth during complicated dental treatment procedures are also of great interest (Romeed et al., 2004; Tom and Eberhardt et al., 2003; Ochiai et al., 2003). Thus, understanding the way in which stresses are distributed in dental structures, and where the highest stresses are concentrated, is important for many types of dental treatments, including applying restorations, designing dental implants, etc.

Background

For many years researchers have been trying to describe the stress state in the human tooth using both experimental and computational methods; there is a wealth of data available on the subject. However, there is no general, systematic means for describing the stress state under loading (e.g. chewing forces or orthodontic devices) for *any* shape tooth under *any* loading conditions; previous work gives a stress description only for a *specific* tooth under a *specific* loading.

Stress analysis of the human tooth

There are basically three different ways in which stress analysis can be performed: analytical, experimental and computational.

Analytical denotes using closed-form mathematical equations to describe the stress state of a structure. In general, biological systems are too complicated for analytical treatment: human teeth are a good example of the complexity of such systems: the geometry is extremely intricate, teeth are composed of 4 sophisticated materials (enamel, dentin, pulp, and the periodontium), and the force distribution due to chewing or dental work varies considerably from tooth to tooth and person to person. In short, there are no analytical stress descriptions of human teeth.

There have been many *experimental* studies of stress in human dental systems. For example, physical stresses can be measured on human teeth that have been extracted (Palamara et al., 2002). Of course, no generalizations can be taken from these because these extractions are always for a specific pathology. In addition, extracted teeth may not behave exactly the same way as teeth in *vivo* (due to dessication and other biological

changes once the tooth is no longer vital and the fact that the tooth is not being supported by the periodontium). There are other types of experimental methods for studying stress distribution, for example, photoelastic analysis (Topbasi et al., 2001; Ochiai et al., 2003; Wang et al., 2004). In this method, a tooth shape is cut out of a plastic material whose transparent luminosity properties change when stressed. Thus, if a light is shone through this material as it is stressed, certain patterns appear showing the stress distribution and concentrations in the material. This method is useful for obtaining very general information about stress distribution, but it cannot take into account the different tooth materials, nor the 3-dimensional nature of teeth. What's more, the experimental process is expensive and time consuming, and any experimental procedure provides a solution for only one particular tooth shape for each experiment and not a general method for describing the stress in *any* tooth.

Stress analysis using *computational* methods would seem to be the most natural way to approach this problem. The experimental process can be simulated and repeated on the computer and be observed in virtual prototyping. It is convenient to change the material or shape properties and obtain the new results. Many researchers have used the computer to analyze dental structures, including human teeth. The primary computational method used for stress analysis today is finite element analysis (FEA). These adapt FEA techniques for studying various dental systems, e.g. the cause of cervical lesion (Tanaka et al., 2003), the shrinkage stress distribution after restoration (Versluis et al., 2004), the role of post rigidity restoration reliability (Lanza at el., 2005), the stresses in dowel-restored teeth (Asmussen at el. 2005), the stress distribution for customized composite post systems (Genovese, at el. 2005), and strains in the marginal ridge

(Palamara et al., 2002), etc. In this method a geometric model is developed and a "mesh" is created by subdividing the geometry into rectangular or brick-shaped elements. In all FEA studies there are four sets of parameters that completely define the model: geometry, material behavior, loading and boundary conditions (BC's). Once the model is completely defined and meshed, a stress analysis is performed and stress distributions are obtained (usually in graphical form).

The definition of the tooth geometry is the first and probably greatest challenge to the stress analyst. Once again, the complexity of the biological structure makes this difficult. Most researchers have developed models which can only be used to solve an individual problem (Borcic et al., 2005; Ausiello et al., 2001; Toparli et al., 2003; Arola et al., 2001; Dejak et al., 2003; Toparli and Sasaki, 2003; Lin et al., 2006; Romeed et al., 2004; Tom and Eberhardt et al., 2003). For example, a FEA model for a mandibular premolar under four concentrated point forces was constructed to analyze the strain in the marginal ridge during chewing (Palamara et al., 2002). This model only gives results for the premolar under concentrated loads. It does not work for other types of teeth (e.g. molar, incisor, etc.) or loading (e.g. mastication, clenching, etc.). Also, to simplify the process, enamel, periodontal ligament, tooth bone, and tooth tissues are not included. In this case the results may be unaffected since only the stress distribution along the marginal ridge is investigated. However, a more general model that could be used for other purposes would be an improvement.

There have been some procedural approaches recently introduced for biomechanical analysis of natural and restored teeth. Chang et al. (2003) developed an integrated method for generating any kind of human tooth geometry model based on the sectioning of a

tooth sample. Because of the complexity of the human tooth shape and structure, this approach involves a sequence of sophisticated techniques as well as special tools. Magne (2006) also developed a systematic method for the generation of finite element models of dental structures and restorations. It is also complex with expert knowledge required. The complicated and highly specialized techniques in these two studies preclude easily repeating them for different geometries, loads and BC's, etc. Lin et al. (1999) developed a method for automatically meshing a 3D FE model for the maxillary second premolar; however, this is not an integrated approach for the whole CAD and FEA process.

Some works create FEA geometry models directly in discretized form (Palamara, 2002; Toparli et al., 2003; Arola et al., 2001; Dejak et al., 2003; Toparli and Sasaki, 2003; Lin et al., 2006; Romeed et al., 2004; Tom and Eberhardt et al., 2003). In this way, the geometry is neither smooth nor accurate. This may cause unreliable results or even no results because of mesh failure. For this reason, constructing a smooth and accurate CAD geometry model and then transferring it for finite element analysis is preferred (Borcic et al., 2005; Ausiello et al., 2001; Magne, 2006; Chang et al., 2003). An expert system (see below) will help the user to generate smooth CAD models using spline curves or surfaces.

Generally, there are two types of data for generating the CAD model: 1) dimensions from measurement or literature (Ausiello et al., 2001; Toparli et al., 2003; Arola et al., 2001; Dejak et al., 2003; Toparli and Sasaki, 2003; Romeed et al., 2004; Rubin et al., 1982; Rubin et al., 1983; Topbasi etal., 2001) or 2) discrete points obtained based on sectioning the tooth sample (Palamara, 2002; Borcic et al., 2005; Lin et al., 2006; Toms and Eberhardt, 2003; Chang et al., 2003) or Micro-CT scanner and segmentation

techniques (Magne, 2006). In this thesis, the expert system will choose the first type of data, i.e. dimensions for model creation. First, a set of representative points will be created based on both the well established shape properties (Lin et al., 2006; Ash, 1984; Ash, 1993; Lindhe and Karring, 1989; Grine, 2005; Schwartz et al., 1996) and the provided dimensions; second, tooth geometry fitting the representative points will be generated. However, the expert system is also applicable for the second type of data input because discrete points can also be taken as the representative points.

Of prime consideration in the development of the stress analysis expert system is the fact that CAD programs and FEA programs are not highly compatible (Magne, 2006; Chang et al., 2003; Rubin et al. 2002; Li and Rubin, 2004); the process of transferring data from CAD to FEA is very difficult and problem specific; for example, FEA doesn't recognize all the entities, such as trimmed curve segments, created in CAD software. In fact, this incompatibility is *the* major challenge for the design and analysis process.

Expert systems

An expert system consists of computer software imbued with the capacity to behave like a human expert in a certain field of knowledge (Liebowitz, 1995). Expert systems exist in many areas of engineering and CAD (Robinson et al., 2001; Chen et al., 2002; Myung and Han, 2001; Song and Im, 1999; Choi et al., 1998; Lee et al., 1998). For example, a system has been developed for determining stress concentrations due to holes in machine parts of various geometries (Robinson et al., 2001); the necessary intuition of an expert to ensure a quality design for a machine part has been incorporated into this program.

Generally, the components for an expert system include a graphical user interface (GUI) and a knowledge based system (Liebowitz, 1995). The GUI makes it possible for users to input information or communicate with the expert system. The knowledge based system is the critical component of the expert system (Lee et al., 1998). It contains the rules for solving the problem using expert knowledge.

Objectives

This thesis describes a project for the development of a computational "expert system" that will automatically perform stress analysis of the human tooth when prompted with sufficient information. Practicing dentists will be able to use this system to optimize treatment for individual patients, and researchers will be able to use it to examine the effects of varying parameters (such as tooth dimensions and chewing forces) on the stress distribution in teeth.

This project provides:

a. a general procedure for generating CAD-FEA tooth models. Smooth and optimized geometry CAD models can be generated and then transferred to the FEA software automatically and seamlessly.

b. GUIs for stress analysis of the human tooth for the use of non-technical dental researchers and practitioners. It is through this GUI that the user will describe the tooth of interest.

c. a knowledge based system for generating CAD-FEA tooth model and perform stress analysis automatically and intelligently.

Tools

The expert system will be implemented by customized software developed on the platforms provided by ProEngineer[1] and Patran/Nastran[2].

Organization

This dissertation includes 4 chapters. This chapter, Chapter I, describes the motivation and related background. It also reviews the previous work related to stress analysis of human teeth. Chapters II and III concentrate on the tooth analysis procedure and system development. Chapter II develops a process for generation of general CAD-FEA models and validates the models by comparison with several previous studies; it also discusses how the materials, geometry and loads affect the stress distribution and the difference between 2D and 3D models. Chapter III develops an expert CAD-FEA system for generating CAD-FEA models and performing stress analysis automatically; it also shows several applications of the system. Chapter IV presents the conclusions drawn from the work and suggests directions for future work.

[1] Parametric Technology Company, Needham, MA, USA, 2006
[2] MSC.Software Corporation, CA, USA, 2006

CHAPTER II

A GENERAL APPROACH FOR STRESS ANALYSIS OF HUMAN TEETH

Introduction

In this chapter a general model for describing the stress state under loading (e.g. chewing forces or orthodontic devices) for *any* shape tooth under *any* loading conditions is presented. This approach is intended to lead to the implementation of computer aided design (CAD) and finite element analysis (FEA) customized codes for automating the stress analysis process. These analyses will move seamlessly between CAD and FEA. The 2-dimensional model developed here is validated by comparison with several previous studies. ProEngineer[3] and Patran/Nastran[4] are used as the CAD and FEA software packages, respectively.

The approach described in this chapter is the first part of a project whose goal is to create an expert system capable of conducting, interactively and automatically, all the tasks involved in the stress analysis of human teeth. The methods developed here can be extended to create 3-dimensional models, and to interpret digital data obtained from image scanning of actual teeth. Dental devices, such as implants, can also be treated with the techniques developed.

[3] Parametric Technology Company, Needham, MA, USA
[4] MSC.Software Corporation, CA, USA

Methods

Step 1. Construction of Parametric models

Each tooth model is determined by the shape and size of the tooth. Tooth shapes are quite consistent for each particular type of tooth (including restorative teeth and tooth implants). The size varies primarily only with the tooth dimensions. Thus, the cross-section parametric models for each tooth type, in a certain direction, can be built using only the tooth dimensions as parameters. This idea makes it possible to generate different types of tooth models automatically by only inputting the information for tooth type, dimensions and cross-section direction.

There are different types of human teeth: central incisor, lateral incisor, canine, first premolar, second premolar, etc. Each type of tooth is composed of five main parts: enamel, dentine, pulp, periodontal ligament and tooth bone. The size and shape of each tooth type, and its component parts, are different. Also, for each tooth type, there are two defined cross-sectional directions: the parallel to proximal (mesial-distal) surface and the parallel to facial (labio-lingual or bucco-lingual) surface. The parametric models for mandibular premolar and lateral incisor in both mesial-distal and buccal-lingual directions and maxillary second molar in mesial-distal direction have been developed in this thesis. Figures 2. 1 and 2. 2 show cross-sections in both directions for the mandibular lateral incisor and first premolar. The methods presented here can be used to generate 2D parametric models for cross sections in either direction for any type of tooth.

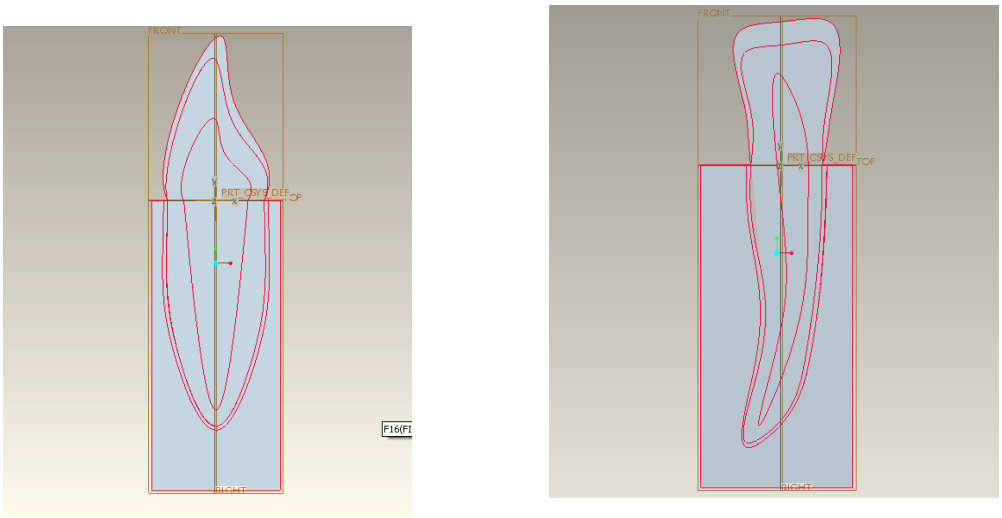

(a) (b)

Figure 2. 1. Cross-sections for manidular lateral incisor in: (a) mesial-distal direction; (b) labial-lingual direction.

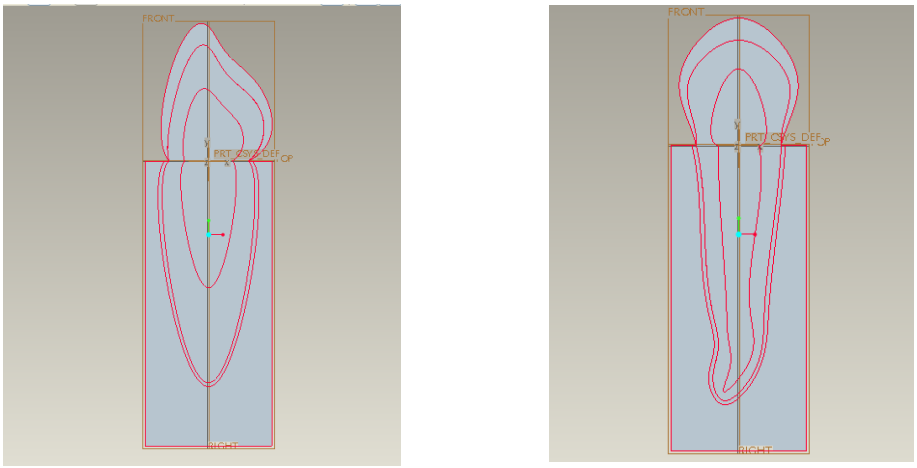

(a) (b)

Figure 2. 2. Cross-sections for premolar in: (a) mesial-distal direction; (b) buccal-lingual direction.

If the size and shape for each tooth part is known, then the geometric model for the tooth is totally determined. Measurements which define tooth size and tooth form can be found in (Ash, 1984; Ash, 1993; Lindhe and Karring, 1989; Grine, 2005; Schwartz et al.,

1996). Generally, there are eight measurements for defining the size of parts of the human tooth (Ash, 1984): length of crown, length of root, diameter of crown, diameter of cervix, thickness of the enamel, thickness of the periodontal ligament, length of bone and width of bone. These dimensions are shown in Figures 2. 3 and 4, in mesial-distal cross section view, for a mandibular first molar and a mandibular first premolar. The form description defines where the tooth curves are convex, straight, sharp, flat, etc. For example, the lingual outline of the crown is convex for a mandibular first molar while it is almost straight for a mandibular first premolar (see Figs 2. 3 and 2. 4).

Each part of the parametric model is generated separately and then all the parts are combined to obtain the model for the whole tooth. In the parametric model there are eight parameters corresponding to the eight measurements listed above. The tooth model is constructed based on the parameters and the description of tooth form. The following method is used for building each part:

1) A sequence of representative points is calculated using the parameters and description of the tooth form for each part. The methods used for calculating the representative points of each tooth type are specific to that particular type. Generally, the more representative points calculated, the more accurate the tooth shape.

2) The representative points are connected together using spline[5] curves to form each tooth part.

3) The whole tooth model is completed by combining all the parts.

For example, the mandibular first molar (shown in Fig 2. 3) is used to describe the construction details for the parametric tooth model. The dimensional values used are averages of values found in the literature; they are listed in Table 2.1. These values can

[5] A piecewise polynomial (parametric) curve.

be modified for different tooth sizes. First, the outline of enamel is generated by: 1) calculating the coordinates of representative points A through H using the size parameters (length of crown, diameter of crown, diameter of cervix and thickness of enamel) and referring to the description of tooth form (i.e. convex or straight, flat or sharp for each side); 2) connecting the calculated points using smooth curves to generate enamel for the first mandibular molar. The emamel is composed of two curves: one connecting points A-B-C-D-E and another connecting points A-F-G-H-E. Similarly, dentine, pulp, periodontal ligaments and tooth bone are generated in turn.

Note that another method for obtaining tooth dimensions could be directly from electronically scanned images. The methods described in this chapter can also be applied to scanned image data.

Table 2. 1. Measurements for mandibular first molar of average size.

	Length of crown, LC [mm]	Length of root, LR [mm]	Diameter of crown, DCr [mm]	Diameter of cervix, DCv [mm]	Maxi-Thickness of enamel, MTE [mm]	Average thickness of periodontal ligament, TP [mm]	Length of bone, LB [mm]	Width of bone, WB [mm]
Madibular first molar	7.5	14.0	10.5	9.0	1.3	0.25	18.	8.
Reference	Ash, 1984	Ash, 1984	Ash, 1984	Ash, 1984	Grine, 2005	Lindhe, 1989	Ash, 1984	Ash, 1984

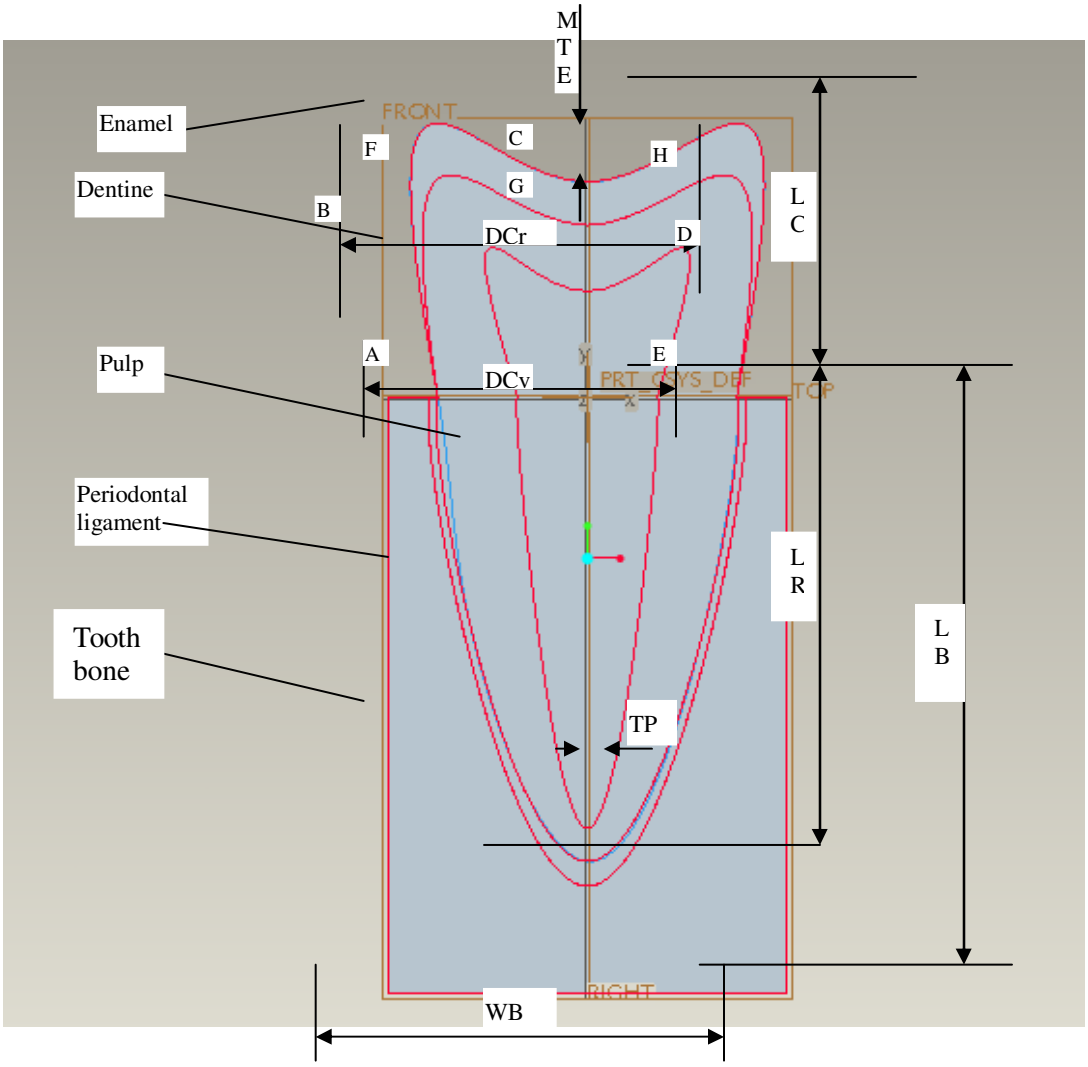

LC — Length of crown
LR — Length of root
LB—Length of bone
DCr — Diameter of crown
DCv — Diameter of cervix
MTE— Maxima Thickness of enamel
TP—Thickness of periodontal ligament
WB- Width of bone

Figure 2. 3. Parametric model of a normal madibular first molar in mesial-distal cross section view.

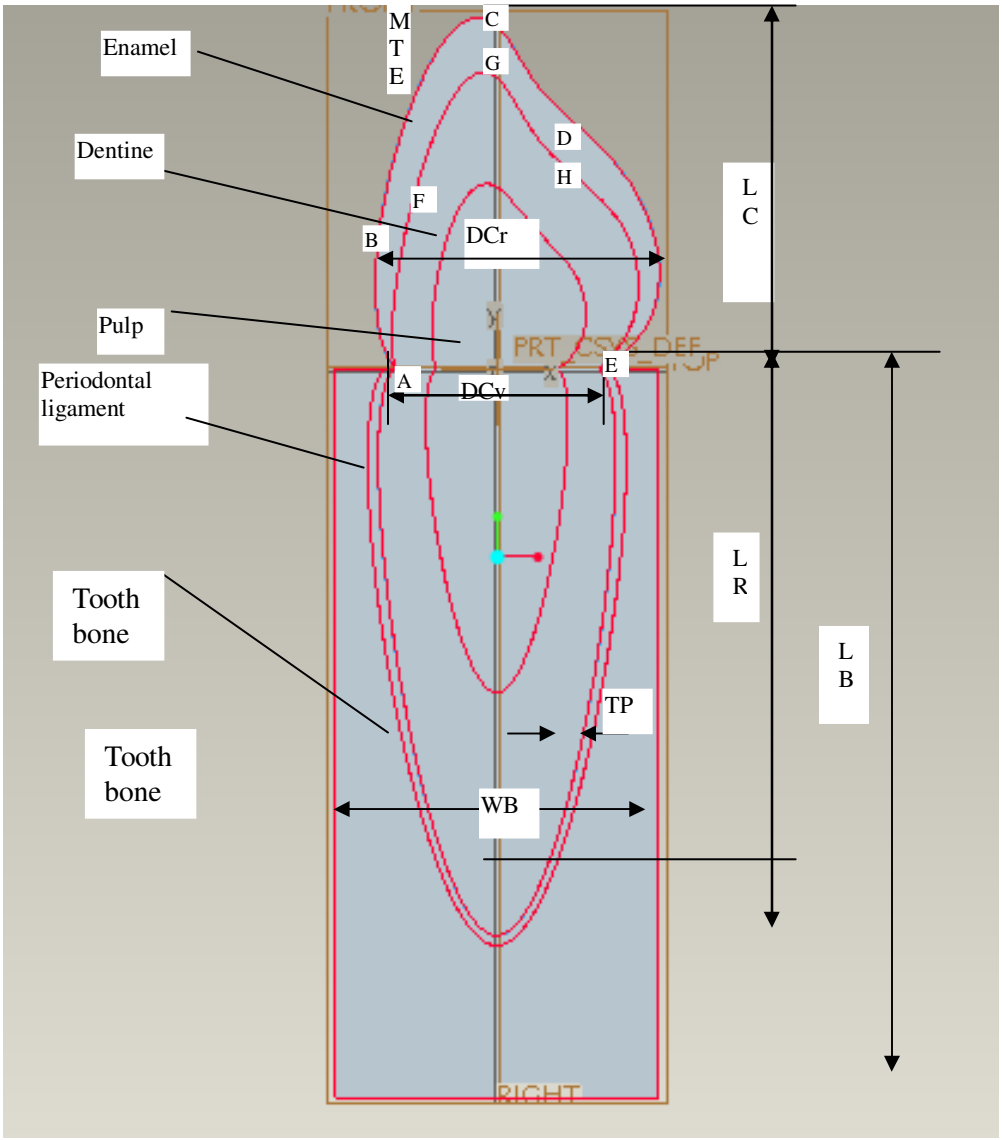

LC — Length of crown
LR — Length of root
LB—Length of bone
DCr — Diameter of crown
DCv — Diameter of cervix
MTE— Maxima Thickness of enamel
TP—Thickness of periodontal ligament
WB- Width of bone

Figure 2. 4. Parametric model of a normal madibular first premolar in mesial-distal cross section view.

Figure 2. 1 shows the parametric models created for mandibular lateral incisors and first premolars in mesial-distal cross section view.

Step 2. Generation of CAD-FEA Compatible Models

Two-dimensional CAD models of human teeth are generated based on the parametric models described above. The following are the requirements for creating a CAD - FEA compatible model:

i. information from the CAD models, i.e., the entities required for performing FEA analysis, such as points, curves and surfaces, etc., must be easily transferable to the FEA software;

ii. automatic meshing of the FEA geometry must be possible; this requires the geometry to be closed and smooth;

iii. Patran/Nastran requires that the element nodes (generated by meshing) along the boundaries between two parts must overlap so that they can be merged by a process called equivalencing. In this way, the parts of the teeth are connected to form a single, continuous object on which stress analysis can be performed.

In light of these requirements, a CAD-FEA compatible model is created as follows:

i. create a new part file using ProEngineer CAD software;

ii. generate each entity (e.g. enamel) that is required for FEA as a single sketch feature in the part file using ProEngineer. These sketch features are generated as described above in the section on construction of parametric models. The following entities must be defined for a 2D finite element model[6]:

    a. surfaces of the parts for meshing;

[6] Any points, curves or surfaces in ProEngineer that will need to be referenced in Patran/Nastran must be defined as individual features in ProEngineer (i.e. they cannot be part of another feature or it will be impossible to have access to them in the FEA software).

b. datum points or curves for defining BC's and other important locations.

iii. save the part file as an IGES[7] file using ProEngineer;

iv. create a new database file using Patran/Nastran FEA software;

v. using Patran/Nastran, import the IGES file to the database file as the FEA geometry;

vi. test the FEA geometry to see if it is suitable for finite element analysis by using mesh and equivalence functions of Patran/Nastran. If it works, the CAD-to-FEA translation has been successfully completed and the analysis phase can proceed. If it fails (usually because the part boundaries do not precisely coincide), return to the second step to optimize the model.

Figure 2. 5 shows a complete CAD model for a mandibular first premolar. This CAD model was then exported to the FEA software as described above and is shown in Fig 2. 6.

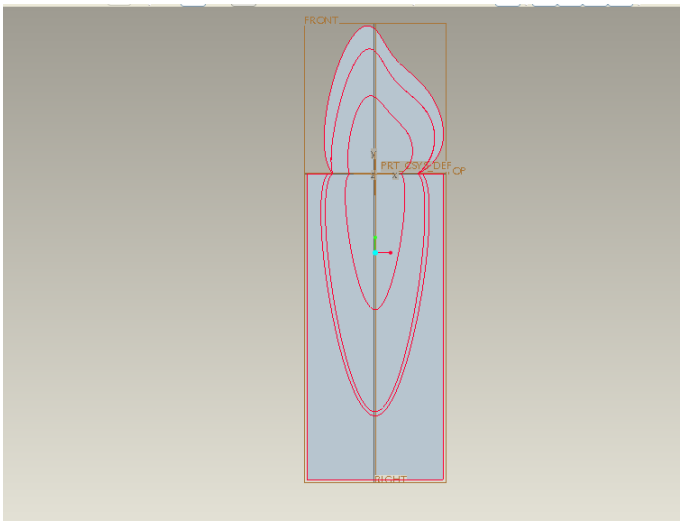

Figure 2. 5. CAD model for a mandibular first premolar.

[7] Initial Graphics Exchange Specification

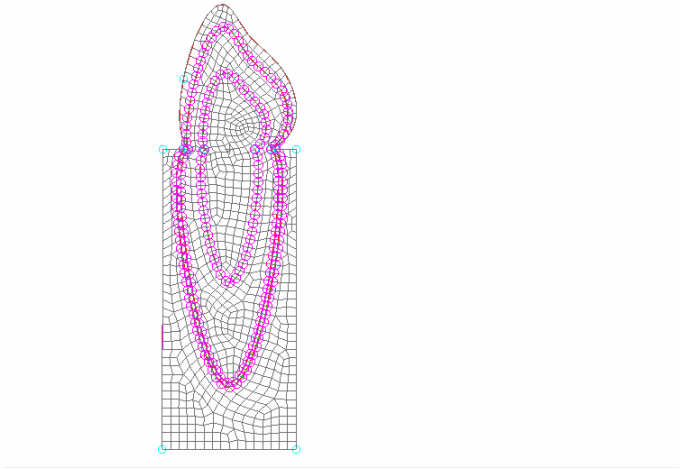

Figure 2. 6. FEA model for a mandibular first premolar after meshing and equavalencing.

Step 3. Definition of the FEA models

The geometries for FEA are ready for preprocessing when the IGES files for the CAD models are successfully imported to the FEA software. The remaining tasks for FEA are:

i. Meshing and equavalencing: The FE model should be ready for meshing since it is imported from a FEA-compatible CAD model. A default element size and type can be used, or the user can customize these if desired.

ii. Adding loads and BC's: All loads on human teeth, whether from orthodontic forces, biting, etc., can be treated as either concentrated or distributed. For human tooth BC's, completely general movements along any directions at any local area can be prescribed. Thus, the loads and BC's for specific situations are easily added.

iii. Defining element properties: The elements for the 2-D tooth models are defined as 2-D solid type, plane strain elements. The material properties (which can be isotropic or anisotropic), including elastic modulus and Poisson's ratio, can be input as desired.

iv. Defining the necessary analysis parameters: Parameters that determine the analysis type and results output, e.g., linear or nonlinear, static or transient, and the output content and format, can be defined according to the specific requirements.

Results-Model Validation

In this section results obtained from analyses performed in Toms and Eberhardt (2003), Chang et al. (2003) and Motta (2006) are compared with similar analyses performed using the new general CAD-FEA modeling approach presented here.

Comparison of results with Toms and Eberhardt (2003).

A 2-D FEA (plane strain) model for a mandibular first premolar in mesial-distal view is generated in Toms and Eberhardt (2003). The model geometry is symmetric about a vertical axis; it includes dentine, bone and PDL (whose properties vary along the tooth roots). Enamel and pulp are not included in the solid model (the enamel and pulp areas are given the properties of dentine). A 1N equivalent load is added at the midpoint of the crown on the buccal side. The base of the tooth bone is fixed. The stress distribution along the PDL under different conditions is determined. The different cases treated include uniform/nonuniform PDL thickness, and linear/nonlinear elastic PDL under extrusive and tip loads.

The case used for comparison with the present CAD-FEA model is a linear elastic tooth with uniform thickness and a PDL under extrusive loading. The FEA model used is shown in Fig 2. 7. This model includes five basic parts: enamel, dentine, pulp, PDL and tooth bone. Table 2.2 includes the material properties used for the above parts. To

approximate the material properties used in Toms and Eberhardt (2003), the material properties for enamel and pulp are assigned the same values as those of dentine. The Young's modulus for the PDL in Toms and Eberhardt (2003) varies along the tooth position. In the present study, the Young's modulus for the PDL is taken as constant. The loads and BC's are similar to Toms and Eberhardt (2003).

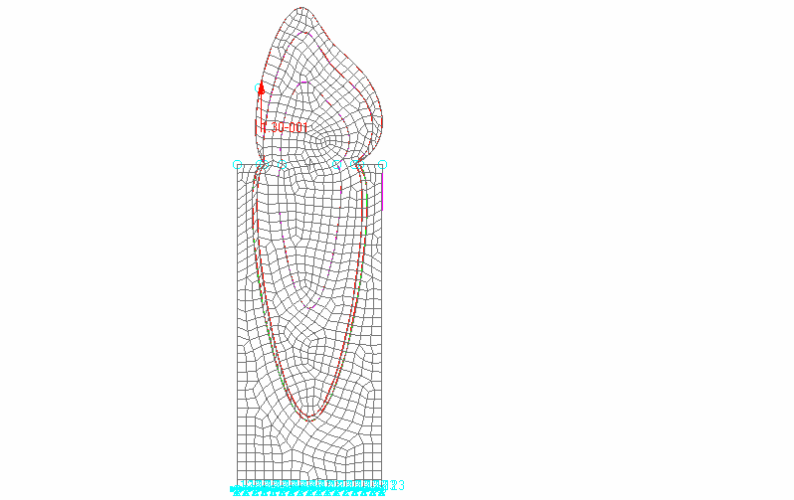

Figure 2. 7. FEA model for a mandibular first premolar with concentrated extrusion loading and fixed base.

Table 2. 2. Material properties for tooth parts in this chapter and Toms and Eberhardt (2003).

Material		Li, Rubin	Toms and Eberhardt (2003)	
enamel	Young's modulus (MPa)	19600	19600	
	Poisson's ratio	0.3	0.3	
dentine	Young's modulus (MPa)	19600	19600	
	Poisson's ratio	0.3	0.3	
pulp	Young's modulus (MPa)	19600	19600	
	Poisson's ratio	0.3	0.3	
PDL	Young's modulus (MPa)	0.25[8]	MP1	0.303
			MP2	0.208
			MP3	0.143
			MP4	0.179
			MP5	0.25
	Poisson's ratio	0.45	0.45	
Tooth bone	Young's modulus (MPa)	13700	13700	
	Poisson's ratio	0.3	0.3	

[8] In Toms and Eberhardt (2003) the Young's modulus for PDL is varied slightly along the root. In this thesis we assume it is a constant value of 0.25.

Figures 2. 8 and 2. 9 and Table 2. 3 present the stress distribution comparisons with Toms and Eberhardt (2003); the lines with squares show the results of the present study and the lines with diamonds show the comparable results from Toms and Eberhardt (2003). It can be seen that there is general agreement for the stress distributions; the shapes of the plots are similar, i.e. the peak values for the stresses occur at the root apex, then the values decline on both sides of the root apex. The stresses are close to zero or below zero at the same positions along the root. Table 2. 3 shows that the magnitudes of the various stresses are of the same order. Some differences are to be expected because:

i. The methods used for generating the geometries were different with Toms and Eberhardt (2003) using a symmetric tooth geometry;

ii. The material properties for the PDL vary along the position of the root in Toms and Eberhardt (2003) (see Table 2.2) while they are constant in the CAD-FEA model.

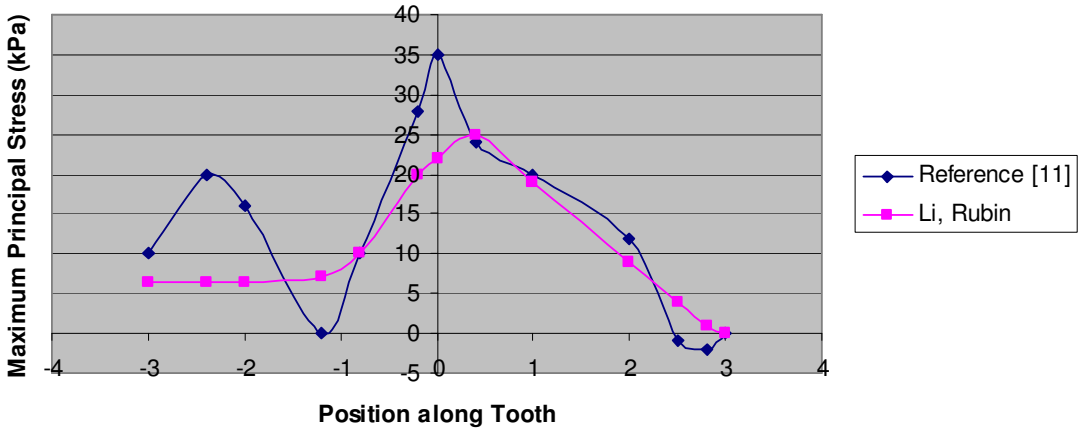

Figure 2. 8. Maximum principal stresses for mandibular premolar subject to extrusive orthodontic force.

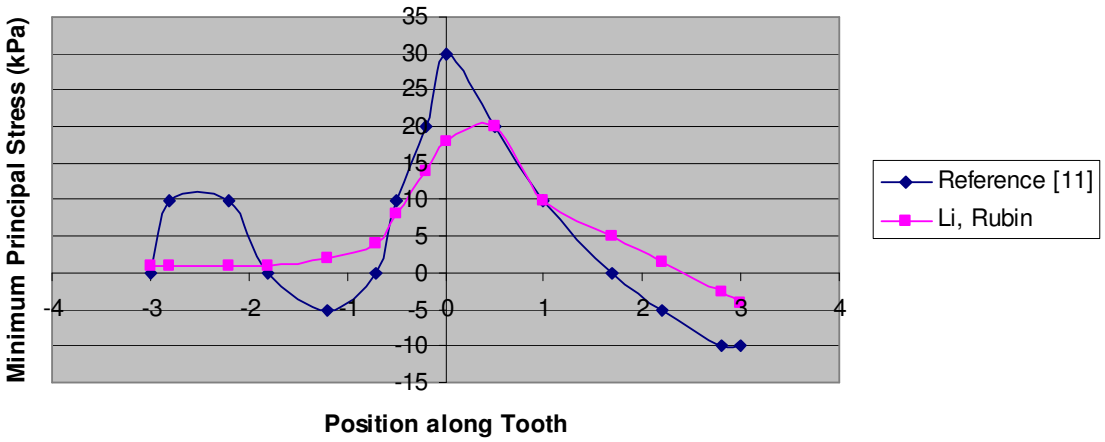

Figure 2. 9. Minimum principal stresses for mandibular premolar subject to extrusive orthodontic force.

Table 2. 3. Average stress across the PDL from tooth to bone as predicted by FE models with uniform PDL thickness in this thesis and Toms and Eberhardt (2003).

		Li, Rubin (kPa)	Toms and Eberhardt (2003), (kPa)
Linguocervical margin	Maximum Principal	-3.99	-2.69
	Minimum Principal	-7.35	-11.6
	Von Mises	2.96	7.75
Apex	Maximum Principal	26.6	36.95
	Minimum Principal	20.3	28.49
	Von Mises	5.92	8.03
Buccocervical margin	Maximum Principal	5.68	13.2
	Minimum Principal	1.11	1.23
	Von Mises	6.00	10.46

Comparison of results with Chang et al. (2003).

The model generated in Chang et al. (2003) is a 3-D model of a human maxillary second molar. Only two parts, dentine and enamel are generated, i.e. the pulp, PDL and bone are not included in the solid model (the pulp area is given dentine properties). A uniformly distributed vertical load of 170 N is applied to the top of the tooth model. The

part which is 2 mm below the enamel is totally fixed. The results for the sectional stress distribution are given in Figure 2. 10(a).

Several CAD-FEA 2-D models of a human maxillary second molar were generated for comparison purposes (Table 2. 4 shows the material properties used in these analyses):

1) Case 1: a model as close to Chang et al. (2003) as possible, i.e. with dentine in place of pulp, and fixed BC's around the tooth base instead of PDL and bone. The loading, BC's, and resulting stress distribution for this model, are shown in Figure 2. 10(b). The maximum stress is 17.3 MPa for the CAD-FEA model while it is 24 MPa for Chang's model. This difference may be due to:

i. the CAD-FEA model being 2-D while Chang's model is 3-D (see discussion below);

ii. the authors were unable to determine exactly how the loads were distributed in Chang's paper, only that the top load was 170 N.

2) Case 2: a model with enamel, dentine and pulp, and fixed BC's around the tooth base instead of PDL and bone. The results are shown in Fig 2. 11(a) where the maximum stress is 35.2 MPa.

3) Case 3: a model with enamel, dentine, pulp, PDL and tooth bone. The results are shown in Fig 2. 11(b) where the stress concentration is 22.1 MPa.

4) Case 4: another model, similar to the last one where the loads were applied in a different way (the loads are applied evenly to 100 nodes); this model better lends itself to automatic load application. The results are shown in Fig 2. 12 where the maximum stress is 25.1 MPa.

Table 2. 4. Material properties for tooth parts in this thesis and Chang et al. (2003).

Material		Li, Rubin				Chang et al. (2003)
		Case 1	Case 2	Case 3	Case 4	
enamel	Young's modulus (MPa)	85000	85000	85000	85000	85000
	Poisson's ratio	0.33	0.33	0.33	0.33	0.33
dentine	Young's modulus (MPa)	19800	19800	19800	19800	19800
	Poisson's ratio	0.31	0.31	0.31	0.31	0.31
pulp	Young's modulus (MPa)	19800	2.07	2.07	2.07	--
	Poisson's ratio	0.31	0.45	0.45	0.45	--
PDL	Young's modulus (MPa)	--	--	50	50	--
	Poisson's ratio	--	--	0.45	0.45	--
Tooth bone	Young's modulus (MPa)	--	--	13800	13800	--
	Poisson's ratio	--	--	0.3	0.3	--

For all of the above cases, stress concentrations of similar magnitude occur on both sides of the tooth. Thus the maximum stress may occur either on the right side (for the first three cases) or the left side (for the fourth case).

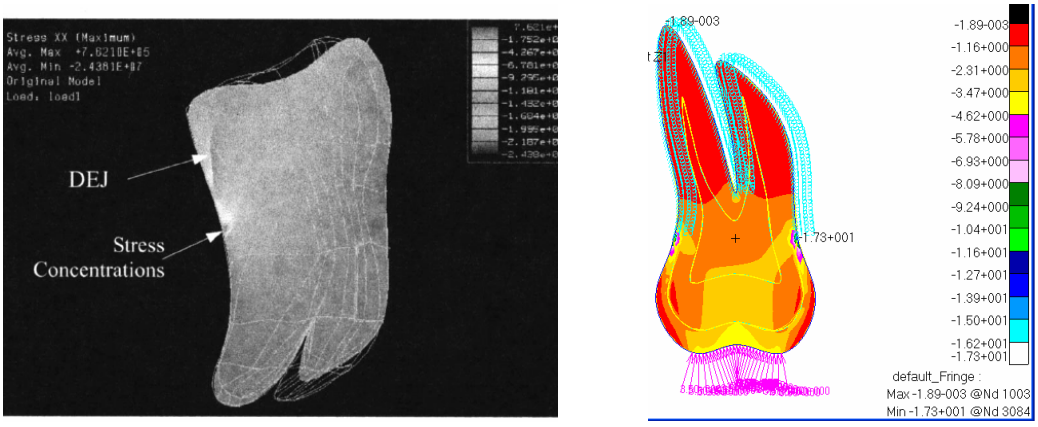

(a) (b)

Figure 2. 10. Minimum principal stress distribution for the maxillary second molar with dentine and enamel obtained from: (a) Chang et al. (2003); (b) Case 1 for the general CAD-FEA model.

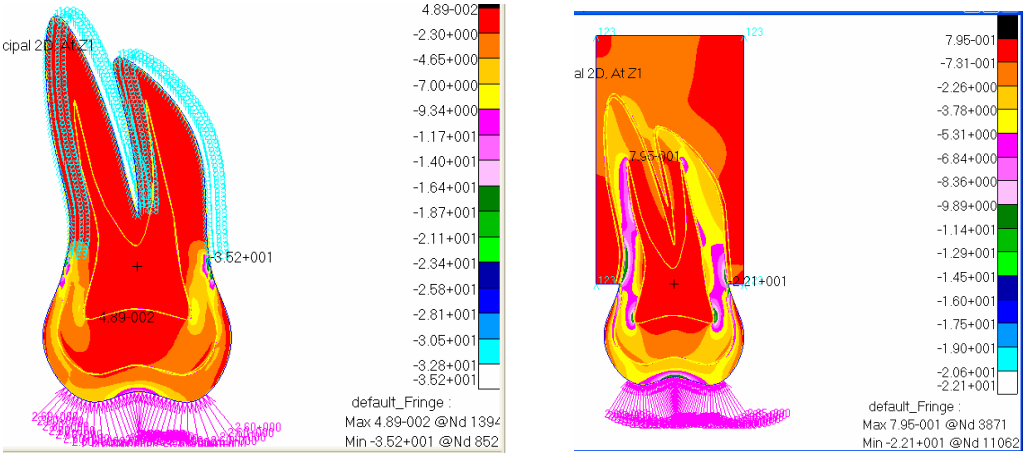

(a) (b)

Figure 2. 11. Minimum principal stress distribution for premolar: (a) Case 2, CAD-FEA model with dentine, enamel and pulp; (b) Case 3, CAD-FEA model with dentine, enamel, pulp, PDL and bone.

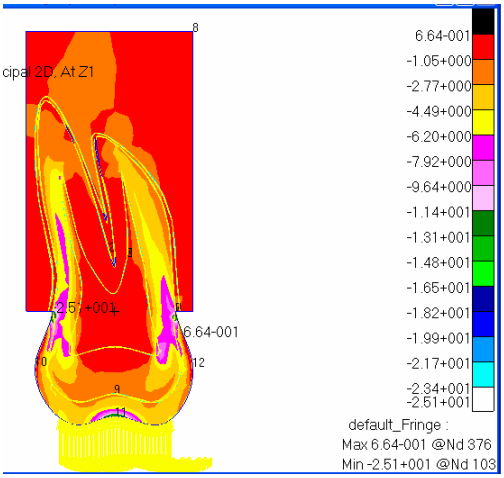

Figure 2. 12. Minimum principal stress distribution for Case 4 of the CAD-FEA model, simulating the distributed loads by equivalent concentrated loads.

Comparison of results with Motta (2006).

Figure 2. 13(a) shows the results of a stress analysis for a mandibular lateral incisor

under a 45 degree load presented in Motta (2006). The PDL thickness is 0.3 mm and the tooth bone is much wider than for the premolar in Toms and Eberhardt (2003). The material properties used for the model are shown in Table 2. 5.

Table 2. 5. Material properties for tooth parts in this thesis and Reference 18.

Material		Li, Rubin	Motta (2006)
enamel	Young's modulus (MPa)	80000	80000
	Poisson's ratio	0.3	0.3
dentine	Young's modulus (MPa)	18600	18600
	Poisson's ratio	0.31	0.31
pulp	Young's modulus (MPa)	2.07	2.07
	Poisson's ratio	0.45	0.45
PDL	Young's modulus (MPa)	50	--
	Poisson's ratio	0.49	--
Tooth bone	Young's modulus (MPa)	13800	13800
	Poisson's ratio	0.26	0.26

Figure 2. 13(b) shows the resulting distribution of maximum principal stresses for a similar model created with the CAD-FEA model. The results are in agreement with Motta (2006) (shown in Fig 2. 13(a).):

1) The locations of the maximum stresses are similar, i.e. at the region under the load and in the cervical region of the lingual face;

2) The stress distribution is similar;

3) The values for the maximum principal stress are of the same order (between 100 and 1000 MPa).

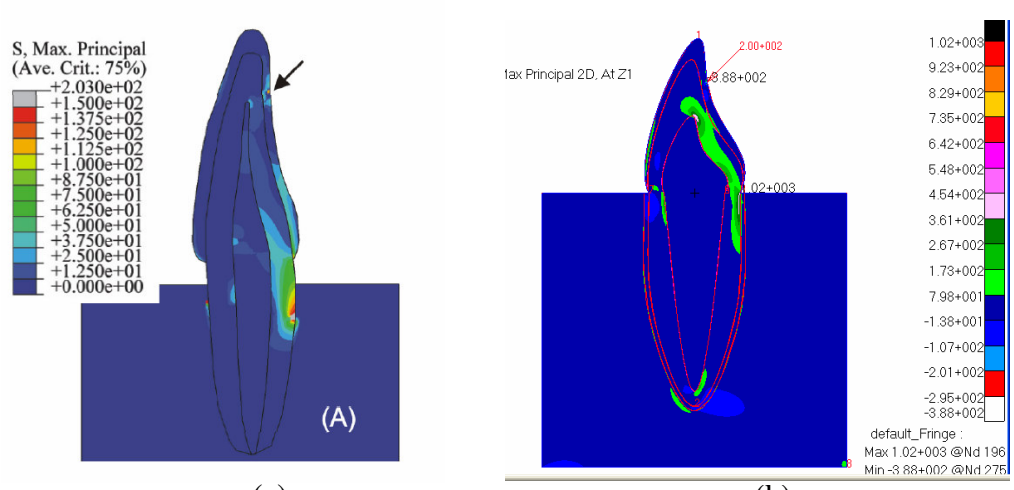

(a) (b)

Figure 2. 13. Stress analysis for mandibular lateral incisor in (a) Motta (2006); (b) general CAD-FEA model.

Discussion

1. Comparing Chang et al. (2003) to the present analyses, it may be seen that the pulp, PDL and tooth bone dramatically affect the stress concentration. The pulp (Fig 2. 10a) raises the stress, since pulp is less rigid than dentine and can't carry as much stress. The PDL and bone (Fig 2. 10b) tend to carry some of the stress and therefore lower the maximum stress. Since these are opposite affects, they cancel each other to some degree, thus yielding a value close to the value that Chang obtained without the inclusion of pulp, PDL and bone.

2. Using evenly distributed concentrated loads or distributed loads on element edges yielded similar results when compared to Chang et al. (2003). Figure 2.14 shows the difference in the models for both cases. The concentrated loads can be more easily incorporated into an automatic interface, but it can be seen that they require the mesh to be more refined and they all act in the same direction.

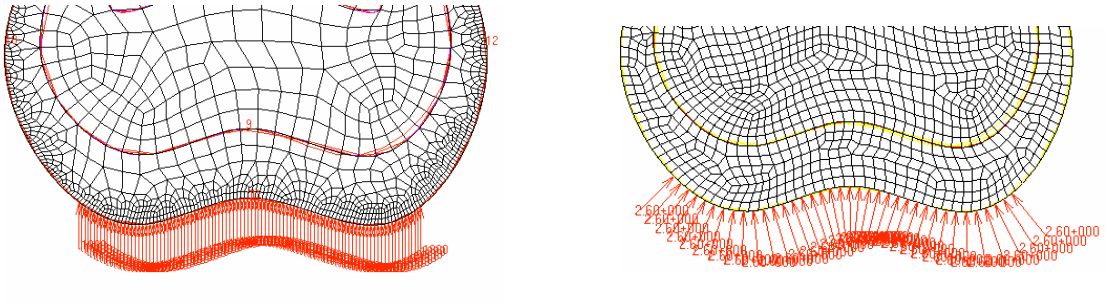

(a) (b)

Figure 2. 14. Tooth loading: (a) concentrated loads evenly distributed on the nodes; (b) distributed loads along the edges of the elements.

3. There are sharp corners at the two ends of the enamel (Fig 2. 15) due to the shape and structure of human teeth. Because of this, the mesh around this area is of poor quality. The maximum stress frequently occurs here (for example, in the maxillary second molar and lateral incisor models). Generally the maximum stress can't be convergent here unless the mesh is refined around the local area. The convergence for the lateral incisor model and the maxillary second molar model will be described below. In the case of the premolar model the stress comparison is along the PDL; since the PDL doesn't contain sharp corners, convergence is not a problem.

The maximum principal stress for the incisor model in Motta (2006) occurs at the corner of the enamel and is convergent at 1.02E3 MPa. For this model, the mesh of both enamel and dentine around the corner of the enamel has been refined (See Fig 2. 15). The percent change for the maximum stress is less than 1% when the refined mesh size changes from 0.05mm to 0.025 mm. So the maximum principal stress is convergent at 1.02E3 MPa for the incisor model. Table 2.6 shows the convergence process for the maximum principal stress.

The minimum principal stress for the second maxillary molar Chang et al. (2003) also occurs at the corner of the enamel and is convergent at 22.1 MPa. The mesh is refined in the same way at the same location as the incisor model. Table 2.7 shows the convergence process for the minimum principal stress.

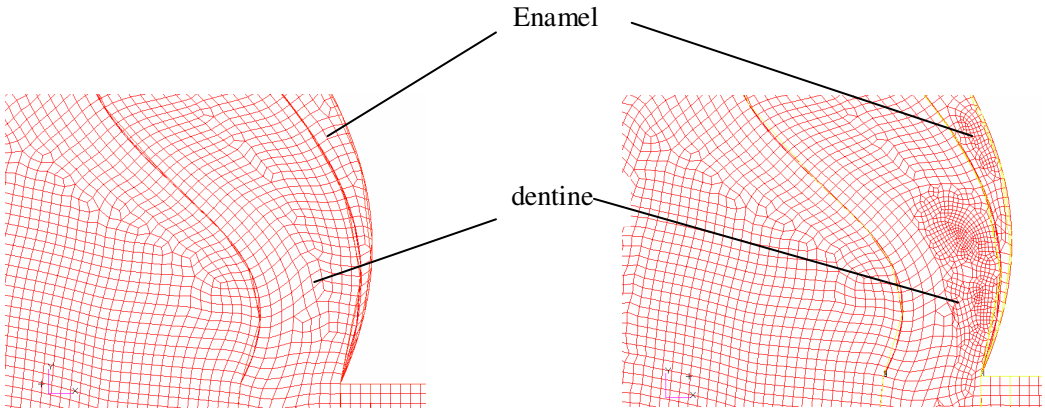

(a) (b)

Figure 2. 15. The mesh around the corner of incisor: (a) without refinement; (b) with refinement.

Table 2. 6. Convergence for the maximum principal stress for incisor (global element size=0.1mm)

Refined mesh size (mm)	Maximum principal stress (MPa)	Percent change
0.1	1.05E3	
0.05	1.03E3	1.9%
0.025	1.02E3	0.97%

Table 2. 7. Convergence for the minimum principal stress for second maxillary molar (global element size=0.1mm)

Refined mesh size (mm)	Maximum principal stress (MPa)	Percent change
0.1	22.4	
0.05	22.1	1.3%
0.025	22.1	0%

For the expert system (see Chapter III), the global or local mesh will be automatically refined further if the difference between the two consequent results is larger than 1%.

4. The differences between 2-dimensional and 3-dimensional models. The comparison of the CAD-FEA model with Chang et al. (2003) brings up the issue of the difference between 2-D and 3-D models for this type of application. Two simple models were created to investigate this issue: a 2-D square and a 3-D cube with the same cross-sectional dimensions and material properties. A thickness of 1mm and an equivalent distributed load of 200 N were applied to both. Table 2.8 shows the details for both models.

Table 2. 8. Definitions for 2-D and 3-D models

	Dimensions (mm)	Total top loads (N)	Load type	BC's	Element type
2D model	10*10	200	Distributed loads	Bottom fixed	2-D solid (plane strain)
3D model	10*10*1	200	pressure	Bottom fixed	solid

Figure 2. 16 shows the results for the minimum principal stresses (i.e. highest compressive stress) for the 2-D and 3-D analyses. The highest value is 29.6 MPa for the 2-D model and 26.8 MPa for 3D model, i.e. the 2-D model yields ~10% higher stress than the 3-D model. Some comments on this result:

i. The comparison with Chang et al. (2003) becomes slightly less good. If we lower the highest stress in the first analysis by 10% we get 16.3 MPa as compared to 24 MPa. It should be remembered here, though, that Chang et al.'s (2003) model was a truly 3-D model in *shape*, so the results would not be expected to be exactly the same. However, order-of-magnitude results are obtained, and the new CAD-FEA model has the advantage of also being able to include pulp, PDL and bone which are not included in Chang et al. (2003).

ii. It is still desirable to develop a 3-D model in order to accurately model actual 3-D geometry and loading conditions out of the plane.

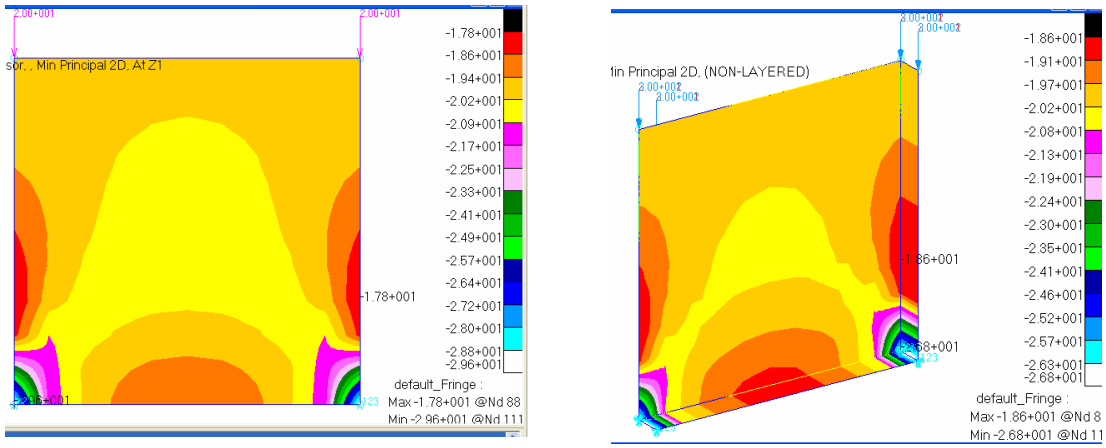

(a) (b)

Figure 2. 16. Minimum principal stress distribution for (a) 2-D model; (b) 3-D model.

5. General discussion of CAD-FEA approach

a. The CAD-FEA model described in this thesis is a general model that can simulate many situations and be used to perform many different tasks.

1. The shape of any type of tooth can be accurately generated when given

enough parameters. There are basically eight parameters used here for defining the tooth shape. For more complicated tooth shapes, such as molars, more parameters may be needed for accurate construction. These parameters can be incorporated into future versions of the code.

2. Both concentrated loads and distributed loads can be simulated at desired locations. For example, the premolar (Fig 2. 7) and incisor (Fig 2. 13) are subjected to concentrated loads while the second molar (Figs 2. 10-12) is subjected to distributed loading.
3. The BC's can be easily defined as needed. Several options will be available for the user to select in the expert system. For example, the bottom of the tooth bone can be fixed for the premolar and incisor (Fig 2. 7 and Fig 2. 13(a) or the root below the enamel can be fixed for the second molar (Fig 2. 10).

b. The analysis process is repeatable. The fact that we can easily vary PDL thickness and tooth bone width, etc., demonstrates the usefulness of the general model developed in the present work. Researchers can run parametric studies to compare the variation of the results as they modify the tooth size, load case, material properties and BC's.

c. The approach presented here is further developed so that the models are generated automatically. Both the ProEngineer and Patran/Nastran software provide platforms for developing codes package for performing the tasks automatically. A graphical user interface is constructed for users to input the necessary information; this will be part of the expert system described in Chapter III.

d. A problem with curve intersection occasionally occurs when the CAD model is created. Sometimes the curves which are generated to create a surface form more than one loop. This will prevent surface creation. The locations of the troublesome points need to be modified slightly so that automatic surface creation can proceed. This process is made automatic and incorporated into the expert system as described in Chapter III.

CHAPTER III

AN EXPERT CAD-FEA SYSTEM FOR STRESS ANALYSIS OF HUMAN TEETH

Introduction

The concept of obtaining the stresses for specific teeth or for parametric studies in a rapid way has been a persistent goal in bioengineering. The previous chapter describes a new, general two-dimensional CAD/FEA tooth model. This chapter presents a computational tool for using that model; it permits dentists with no engineering expertise to obtain stress concentrations and distributions for various dental applications. Two applications are presented to show how the expert system works. The techniques and theories developed and applied here can be expanded to provide automatic stress analyses for many other applications as well.

The expert system

Special problems

In all FEA-to-CAD systems there are specific issues that must be dealt with that are unique to the particular application. Below are listed some of these problems. Although they apply specifically to the tooth analysis problem, they are typical of the issues that must be dealt with in developing any automated CAD-to-FEA process.

1. Creating a general two-dimensional CAD geometry for any type of tooth in either cross-section direction. Tooth geometries are irregular and each type of tooth has a different shape. Accurate, user desired tooth geometries, must be generated once the tooth type, direction and dimensions are decided, through the use of GUIs.

2. Optimizing the geometry to ensure that the CAD model is reasonable. Tooth parts are represented by 2D surfaces. The outline curves of the surfaces should form a single closed loop, i.e., there should be no intersection between the outline curves that form a tooth part. Otherwise, the surface that represents the tooth part can't be generated. Curve intersections might occur at the sharp corners of the ends of tooth enamel, as illustrated in Figs 3. 1 (a) and (b). Then the outline curves for enamel will be muti-looped and it will not be possible to generate a surface for the enamel. In this case, the outline curves for enamel must be modified to avoid curve intersections.

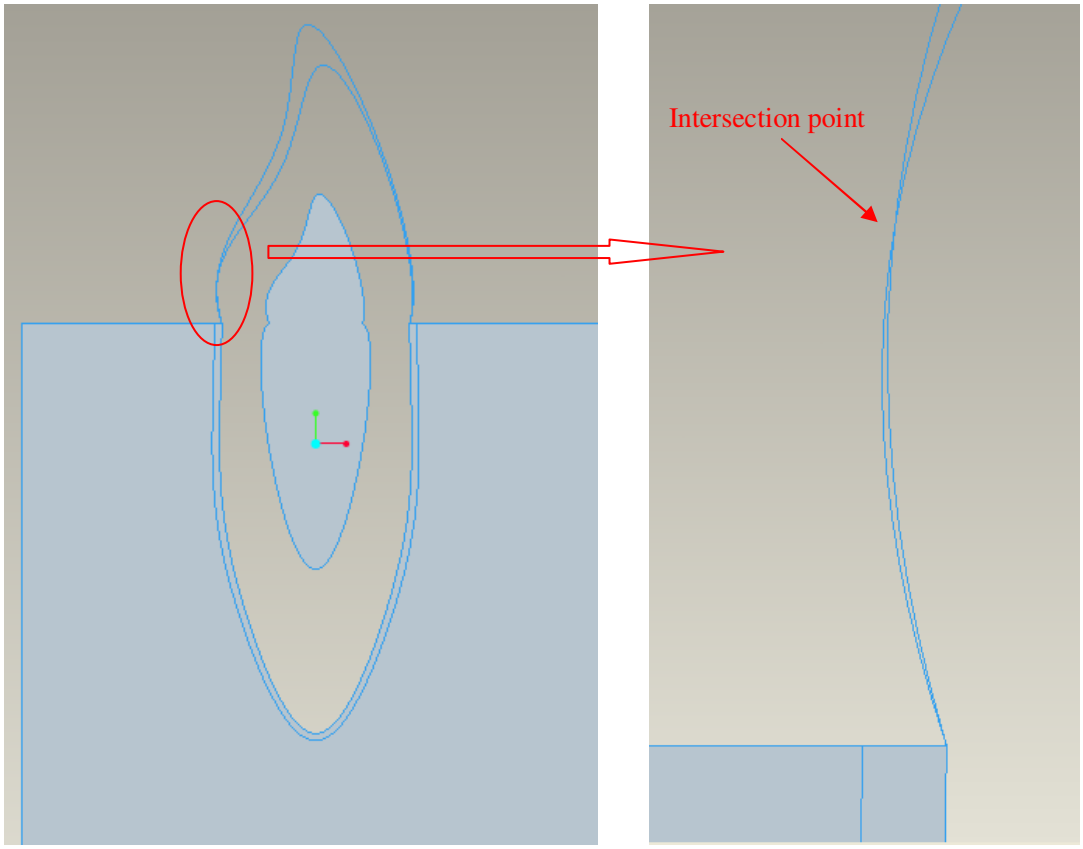

(a) (b)

Figure 3. 1. (a) Regular; (b) enlarged image for tooth geometry with intersection points

3. Deciding the initial FEA mesh size and meshing the tooth geometry. A sufficient number of elements are required for FEA convergence. Also, models with different dimensions need different mesh sizes. Initial mesh size should be decided according to tooth geometry and an appropriate mesh type must be defined.

4. Providing an automatic method for users to define the FEA model, including adding loads, BC's and material properties. The input or modification of values

and locations for each type of load and boundary condition should be convenient. Also, there are several typical applications for tooth stress analysis such as orthodontic and occlusion applications. Load types and BC's for these, and other applications, should be available in a menu for selection by the user.

5. Conducting mesh convergence testing. Mesh refinement and reanalysis must be available and the analysis results for each refined mesh at sensitive locations must be presented to be sure that convergence has been attained. Loads are usually applied to nodes and elements. The existing nodes and elements will disappear and new ones will be generated when refining the mesh for convergence testing. It is necessary to ensure that the loads are applied to the same location before and after mesh refinement.

6. Displaying the results clearly. A variety of result data, such as stresses and displacements, must be easily accessible; this would include graphs showing stress contour fringes, or text reports.

System configuration

The developed system[9] creates the CAD-FEA model and performs stress analysis on human teeth by hierarchically applying the rules stored in the knowledge-base; the system configuration is illustrated in Fig. 3. 2. The expert system was constructed of two modules each containing the tasks described below.

CAD module: creates CAD geometry, optimizes geometry and exports geometry from CAD program (ProEngineer)

[9] Refer to Appendix E for the software package created for the expert system.

FEA module: imports geometry to FEA software (PATRAN/NASTRAN), creates FEA model, analyzes the model, checks convergence and displays results.

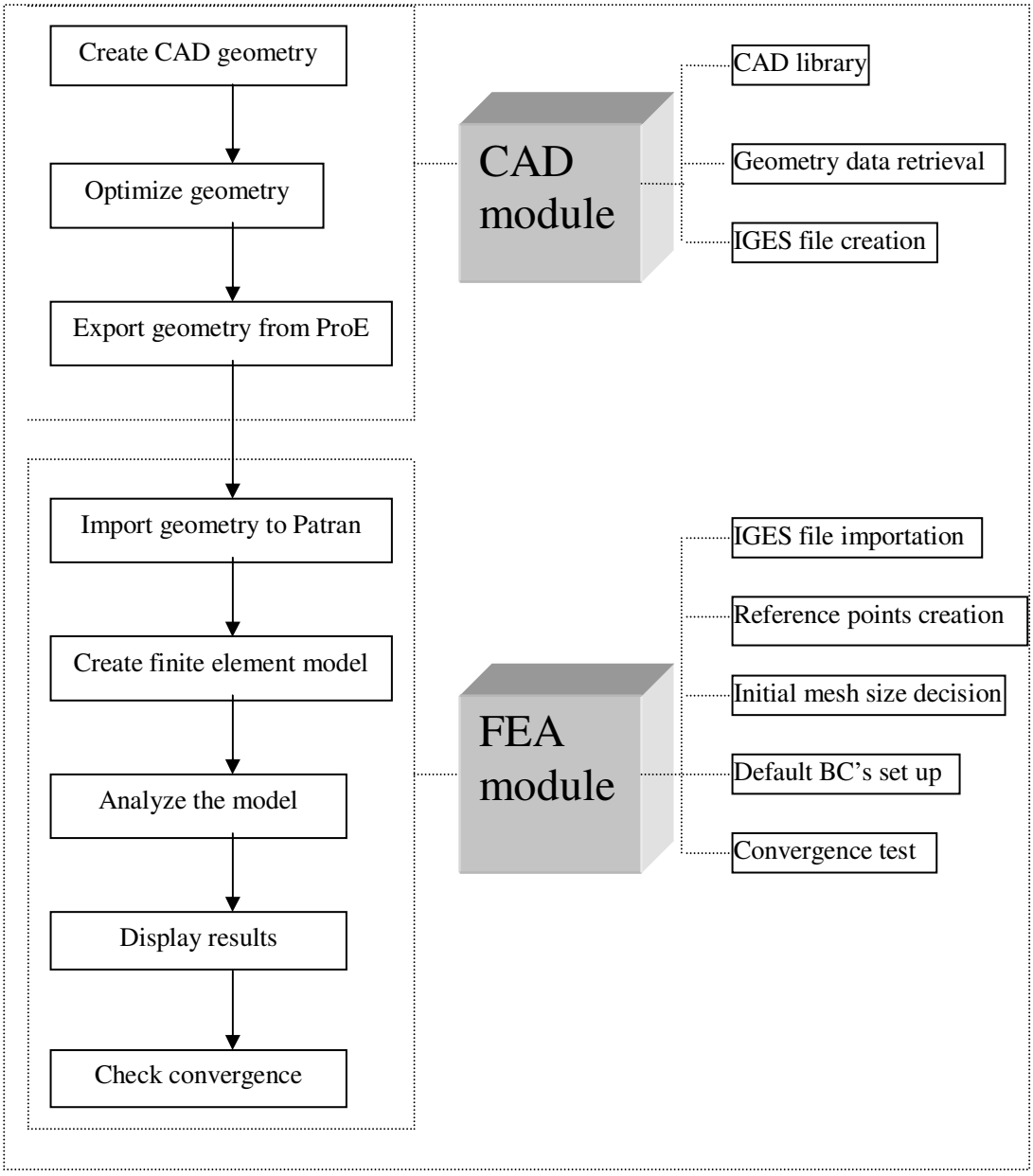

Figure 3. 2. Configuration of the expert system.

Knowledge base

Create CAD geometry: The CAD tooth model is designed based on the geometry information input: tooth type, cross-section direction and dimensions. A CAD library has been constructed which includes parametric tooth models of several different tooth types (incisor, premolar, and maxillary second molar) in several directions (mesial-distal and labial-bucal cross sections). The different tooth models with their default dimensions and cross-section directions are shown in Table 3.1. The system will generate a proper model when the geometry information is input. Five surfaces will be generated for representing five main tooth parts (enamel, dentine, pulp, PDL and bone). More specifically, when tooth type and direction information are input, the related parametric model for that type of tooth, in the desired direction, is selected from the CAD library to create the tooth geometry. First, the 2D closed curves that outline the tooth parts are generated; second, the system optimizes the geometry (see details in next paragraph); third, the 2D curves will be located in 3D space using a translation matrix; finally, the surface for each tooth part is generated by filling the closed curves.

Optimize geometry: The system retrieves information on the created spline curves, expressing them as piece-wise parametric cubic curves[10], and then checking if there is a curve intersection between them[11]. If an intersection exits, the model will be optimized. Intersections are removed by adding interpolation points to modify the local shape of the curves.

[10] Refer to Appendix A for expressions for spline curve and Appendix F for an example of the retrieved data.
[11] Refer to Appendices B and C for the algorithms and Appendix F for an example of the calculated results.

Table 3. 1. Default dimensions for different tooth models (refer to ChapterII for more details).

Tooth model	Length of crown (mm)	Length of root (mm)	Diameter of crown (mm)	Diameter of cervix (mm)	Max-Thickness of enamel (mm)	Thickness of PDL (mm)	Length of bone (mm)	Width of bone (mm)
Incisor in mesial-distal direction	10.5	14.0	6.5	6.0	1.3	0.25	18.0	20.0
Incisor in labial-lingual direction	8.0	15.5	4.8	4.0	1.3	0.25	18.0	8.0
First premolar in mesial-distal direction	9.0	14.0	7.0	5.0	1.3	0.25	18.0	8.0
First premolar in labial-lingual direction	7.5	15.0	7.0	5.0	1.3	0.25	18.0	8.0
Secondary molar in labial-lingual direction	6.5	12.0	9.0	7.0	1.3	0.25	16.0	10.0

Export and import geometry: The CAD model is exported from ProE by creating an IGES file and then is imported into Patran as a FEA geometry.

Create FEA model: First, the initial mesh size is determined and then the mesh is created based on the FEA geometry. The system calculates the whole area of the tooth geometry, and then decides the initial global element size for the model. Table 3. 2 shows different area ranges and corresponding global mesh sizes. Second, load types, BC's and element properties are defined. Third, to ensure that the loads are applied at the same location(s) before and after refining the mesh, reference points are generated and forces

are applied to the closest nodes around those points, or distributed loads are applied to the element edges between the points. The locations of the reference points along the outline of the enamel layer can be specified by the user through a parameter—the "space ratio"; this is the ratio of the two lengths which have been segmented by the reference point. Fourth, the types, values and locations of loads and BC's can be defined through user GUIs. Default BC's are provided for typical applications. Fifth, material properties for each tooth part are defined by the user through GUIs (default values are also available, as shown in Table 3.3). For all the tooth parts, the element type is defined as a 2D solid, and a plain strain model is used.

Table 3. 2. Global element size for different ranges of cross-section area.

Cross-section area (mm^2)	0-50	50-100	>100
Global element size (mm)	0.2	0.4	0.8

Table 3. 3. Default values for material properties of each tooth part.

	Enamel	Dentine	Pulp	PDL	Bone
Young's modulus (MPa)	19600	19600	19600	0.25	13700
Poisson's ratio	0.3	0.3	0.3	0.45	0.3

Analyze the FEA model and access the results: The completely defined FEA model is analyzed employing Nastran codes. The analysis results are then imported to Patran for display.

Result display: After running the analysis, the stress results (Von mises, maximum principal and minimum principal) can be obtained in the form of fringe contours or a text report. X-y scatter graphs of the stresses along the PDL are automatically provided since the shape of the PDL is a long narrow belt making it difficult to observe the stress distribution from fringe graphs.

Check convergence and refine the mesh: There are four steps for automatic user initiated convergence testing: first, the FEA model is remeshed with element edge length half the size of the previous mesh; second, load locations are redefined, since loads are applied to nodes and the nodes are changed during remeshing. Third, the model is analyzed and the results accessed as before; fourth, a "convergence.out" file is generated; this file shows the convergence of the stresses along the points where stress concentrations usually occur. Users can observe the results to see if further mesh refinement is necessary. Since stresses at geometry points can't be retrieved directly, the values of the stresses shown are average values for nodes near the geometry points. However, the process of locating the high stresses for convergence testing has not been automated in this work, i.e. presently users must determine the coordinates of the geometry points by observing the stress distribution on the stress fringe forms.

Graphical User Interface

Below is a detailed description of the GUI that a user will step through, including model creation, completing the stress analysis process and obtaining graphical output results for evaluation.

The user opens the ProEngineer software. The software modules developed as part of this project must be located in the CAD/FEA work directory (see Appendix D).

CAD customization menu bar—"Tooth CAD": This toolbar menu contains three menu selections, as illustrated in Fig. 3. 3, more GUIs will pop up when the menu buttons are clicked:

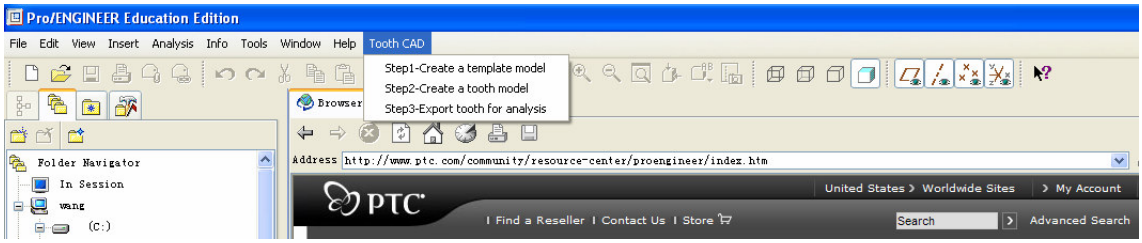

Figure 3. 3. ProEngineer customized application main menu.

Step1-Create a template model: An initialized CAD model will be generated in this step. The initialized CAD model contains all the features (such as default front, back and top planes etc.) that are essential for constructing a CAD model. No windows will pop up when the button is selected since no input is required for this step.

Step 2-Create a tooth model: Tooth type and dimensions will be defined and a tooth model will be generated in this step. Two or three GUIs will appear for defining the tooth geometry and naming the model, respectively: i) **Tooth Geometry Information Input Window** (Fig 3. 4(a)) will pop up once the menu button is selected. This window is used for selecting tooth type and tooth cross-section direction, inputting tooth dimensions, and then creating tooth geometry. The default values for tooth dimensions will be set and displayed once the tooth type and cross-section direction are decided.

Users can either accept or modify these values. The tooth geometry will be generated once the "ok" button is clicked. ii) **Curve Intersection Information Window** (Fig 3. 4(b)) will appear if a curve intersection exists within a tooth part. The coordinates for the intersection point are displayed. The tooth geometry can be modified to avoid the curve intersection once the "ok" button is clicked. iii) **CAD model name input panel** (Fig 3. 4(c)) will appear when the CAD model is completely generated. A file extension of ".prt" will be added automatically to the input name.

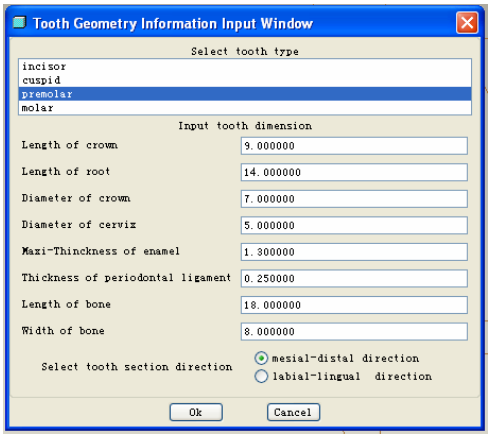

(a)

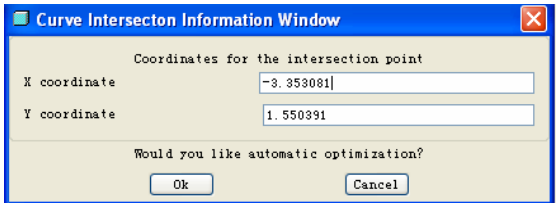

(b)

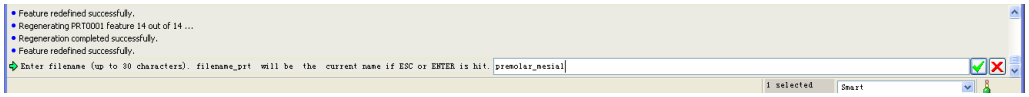

(c)

Figure 3. 4. GUIs for CAD model creation: a) Tooth Geometry Information Input Window; b) Curve Intersection Information Window; c) CAD model name input panel.

Step 3-Export tooth for analysis: The tooth model will be exported as an IGES file in this step. Two GUIs will appear for selecting the directory and inputting the name for the IGES file: **i) Select Directory dialogue box** (Fig 3. 5(a)) **ii) Export IGES file dialogue box** (Fig3. 5(b)). The default CAD part file name will be taken as the IGES file name. Users can either accept or modify the current file name.

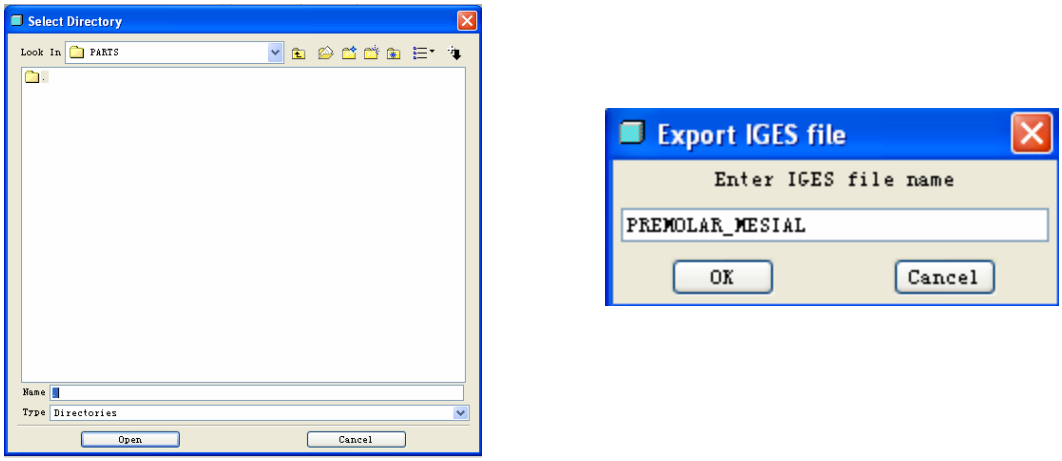

(a) (b)

Figure 3. 5. GUIs for CAD model exportation: a) Select Directory dialogue box; b) Export IGES file dialogue box.

The user opens the PATRAN software. The PATRAN/NASTRAN modules developed as part of this project must be located in the CAD/FEA work directory (See Appendix D).

FEA customization menu bar—"Tooth FEA": This toolbar menu contains ten menu buttons, as illustrated in Fig 3. 6; more GUIs will pop up when the menu buttons are clicked:

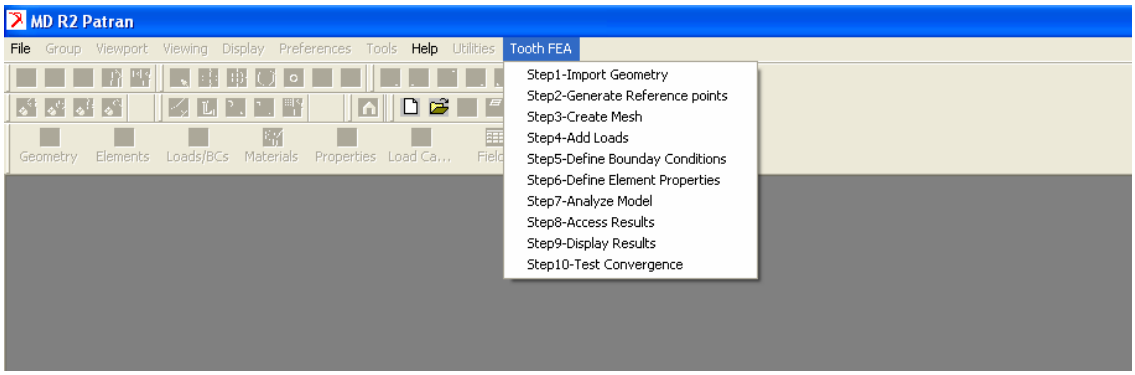

Figure 3. 6. Patran customized application main menu.

Step1-Import Geometry: The tooth geometry will be imported into the FEA software in this step. The **Import Geometry Window** (Fig 3. 7) will pop up when the menu button is clicked. This window is used for inputting the name of a new database file, selecting the IGES file and importing it into the FEA software. The **Select File** dialogue box will pop up when the **Select File** button is clicked.

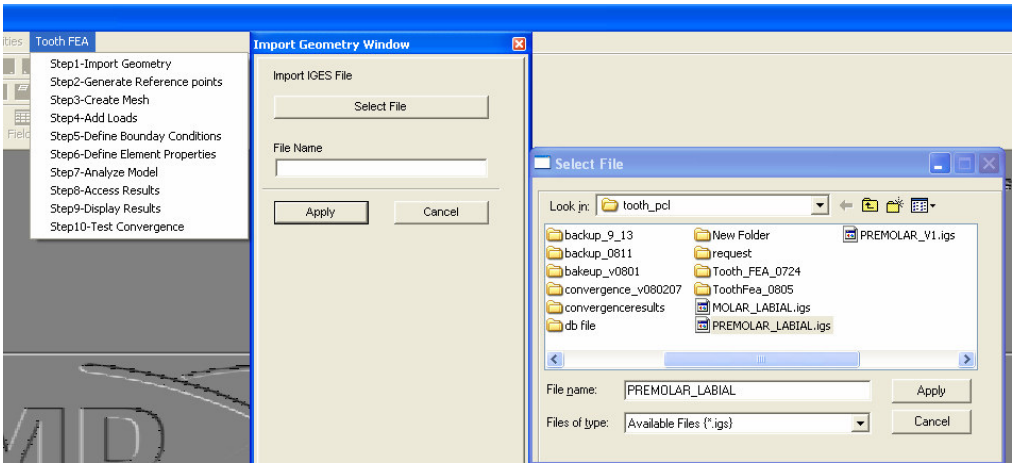

Figure 3. 7. GUIs for Step 1: Import Geometry Window and Select File dialogue box.

Step 2-Generate Reference Points: The reference points for defining the loads and BC's will be created in this step. The **Generate Reference Points Window** (Fig 3. 8) will

pop up when the menu button is clicked. This window is used for inputting the "space ratio" value- the ratio of the two lengths along the enamel outline which have been segmented by the reference point.

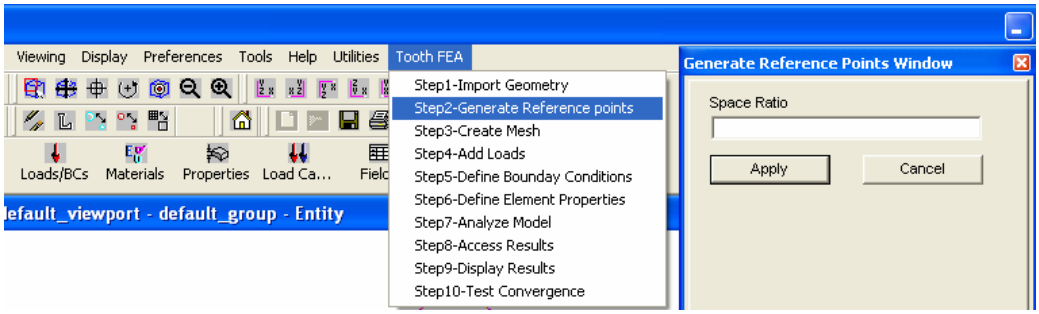

Figure 3. 8. GUI for Step 2: Generate Reference Points Window.

Step 3-Create Mesh: The FEA geometry will be meshed in this step**.** The system will decide the mesh size based on the whole area of the tooth geometry. No window will open when the menu button is clicked since no input information is required.

Step 4-Add Loads: Loads will be added to the tooth model in this step. The **Add Loads Window** (Fig 3. 9(a)) will pop up when the menu button is clicked. This window is used for choosing load types: **Concentrated Forces** or **Distributed Loads**. The **Create Force Form** (Fig 3. 9(b)) or **Create Distributed Loads Form** will pop up when the load type is selected. The load values and locations can be input through these forms.

Step 5-Define boundary conditions: BC's will be defined in this step. The **Define Boundary Conditions Window** (Fig 3. 10(a)) will pop up when the menu button is clicked. This window is used for selecting boundary condition type: **Constraints on Nodes** (Fig 3. 10(b))**, Constraints on Surface Edges, Default Orthodontic Constraints** and **Default Occlusion Constraints.** The **Create Constraints on Nodes Form** or

Create Constraints on Edges Form will pop up when the first two types are selected**.** The constraints values and locations can be input through these forms. No inputs are required for the last two types since default BC's will be automatically defined when they are selected.

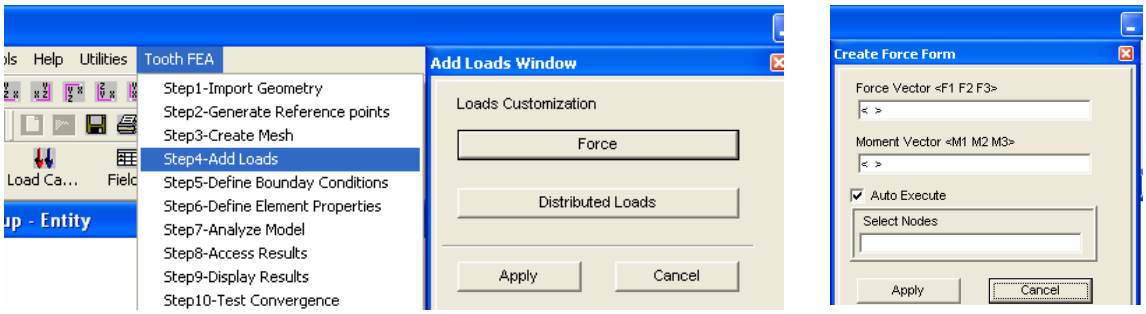

(a) (b)

Figure 3. 9. GUIs for Step 4: (a) Add Loads Window; (b) Create Force Form.

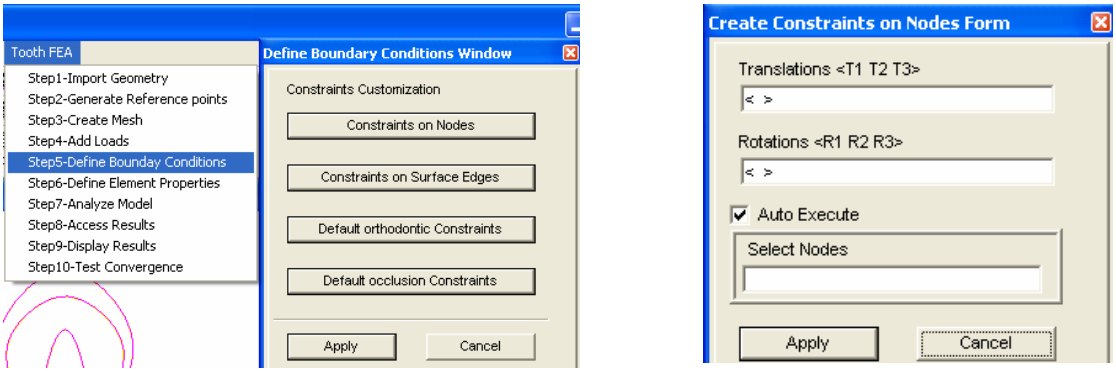

(a) (b)

Figure 3. 10. GUIs for Step 5: (a) Define Boundary Conditions Window; (b) Create Constraints on Nodes Form.

Step 6-Define Element Properties: Element types and material properties will be defined in this step. The **Define Element Properties Window** (Fig 3. 11(a)) will pop up when the menu button is selected. This window is used for selecting tooth parts: **Enamel, Dentine, Pulp, PDL** and **Tooth Bone**. The forms such as **Input Properties for Enamel**

(Fig 3. 11(b)), etc**.** will pop up when a tooth part is selected. These forms are used for inputting material properties such as elastic moduli and poisson's ratios for a selected tooth part. Default values are provided. Users can either accept or modify them. No input is required for element type since the element type used for all tooth models is 2D solid.

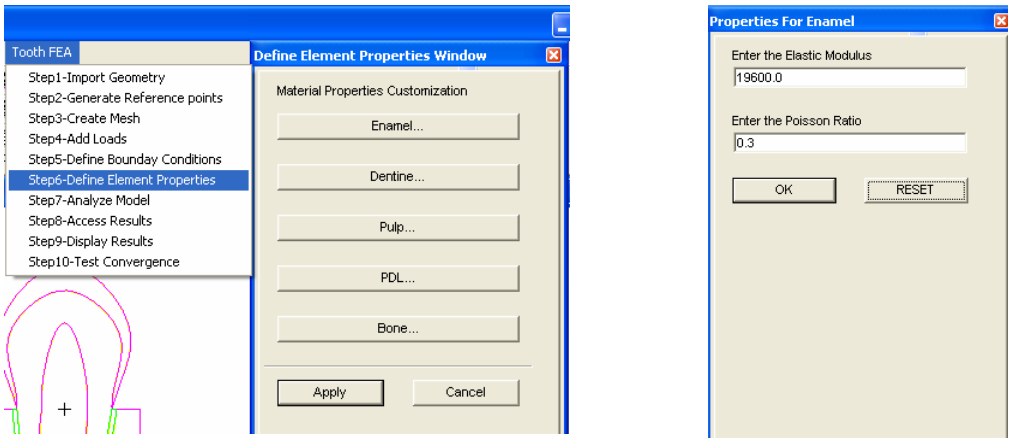

(a) (b)

Figure 3. 11. GUIs for Step 6: (a) Define Element Properties Window; (b) Properties for Enamel form

Step 7-Analyze Model: The FEA model will be analyzed in this step. The **Analyze Model Window** (Fig 3. 12) will pop up when the menu button is clicked. This window is used for inputting a job name.

Step 8-Access Results: The analysis results will be imported from Nastran to Patran in this step. No input is required. The system will search the results by referencing the above job name.

Step 9-Display Results: Various options are provided for displaying the analysis results in this step. The **Display Results Window** (Fig 3. 13(a)) will pop up when the

menu button is selected. This window is used for selecting results type: **Stress, Displacement or Constraint Forces**. The **Display Stress Window** (Fig 3. 13(b)) will pop up when **Stress** is selected. Users can further define the result form (fringe, graph or report), and quantity (Von mises, maximum or minimum principal stress).

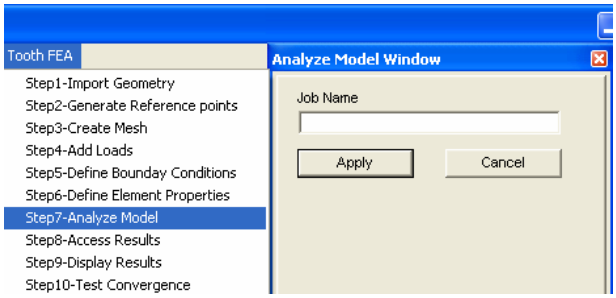

Figure 3. 12. GUIs for step 7: Analyze Model Window.

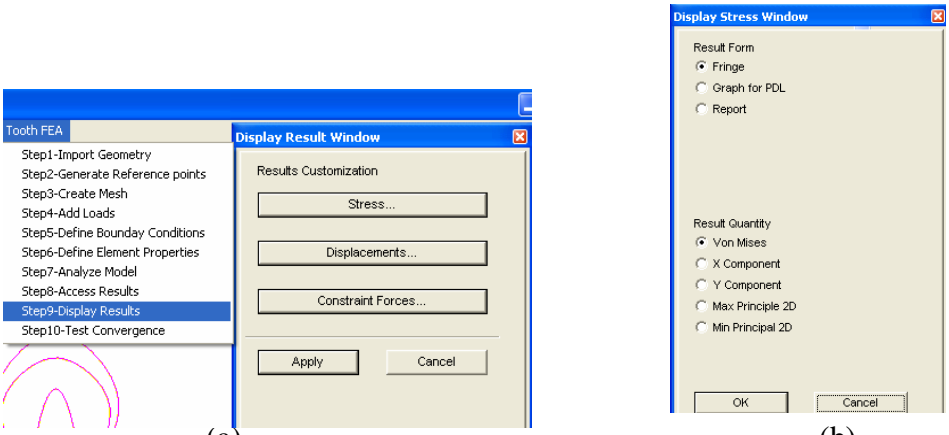

(a) (b)

Figure 3. 13. GUIs for Step 9: (a) Display Result Window; (b) Display Stress Window.

Step 10-Test Convergence: The mesh will be refined and a convergence test will be performed in this step. The **Test Convergence Window** (Fig 3. 14) will pop up when the menu button is selected**.** The Window contains two buttons: **Refine Mesh** and **Create Convergence File**, which should be selected in turn. No input is required for these two sub-steps.

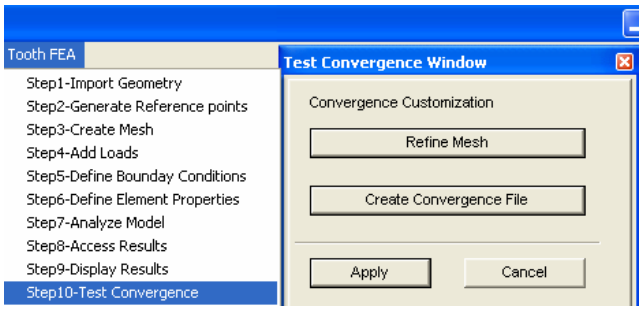

Figure 3. 14. GUIs for Step 10: Test Convergence Window.

Applications

Orthodontic application: The expert system is applied to a mandibular first premolar under an orthodontic extrusive force of 100 N. In this application, the tooth model is generated and analyzed in the mesial-distal direction.

1. CAD model creation

   The CAD model for a mandibular first premolar is shown in Fig 3. 15. The following are the input geometry data:

   Tooth type: mandibular first premolar

   Cross-section direction: mesial-distal direction

   Tooth dimensions: default dimensions for first premolar in mesial-distal direction (refer to Table 3. 1.)

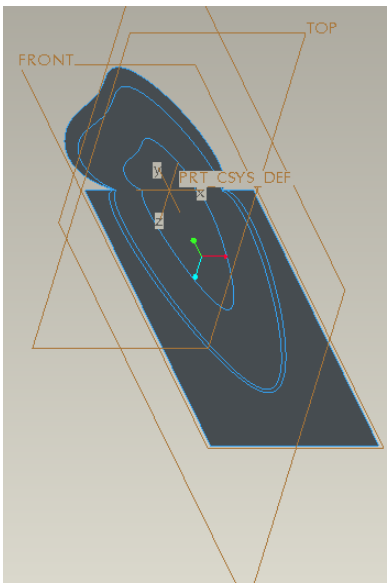

Figure 3. 15. Two-dimensional CAD model for mandibular first premolar in mesial-distal direction.

2. FEA model definition

A reference point is generated for adding a concentrated force: point 11 with space ratio 3, as illustrated in Fig 3. 16(a).

The initial global element size for the premolar is 0.8 since its whole area is about 190 mm^2; the mesh is illustrated in Fig 3. 16(b).

The load type selected is "Force." A force of 100N is applied to the nodes closest to point 11, as illustrated in Fig 3. 16 (c).

“Default orthodontic constraints” is selected as the boundary condition, as illustrated in Fig 3. 16(c). This fixes the bottom of the tooth bone.

Default material properties are taken as the material properties, given in Table3. 3.

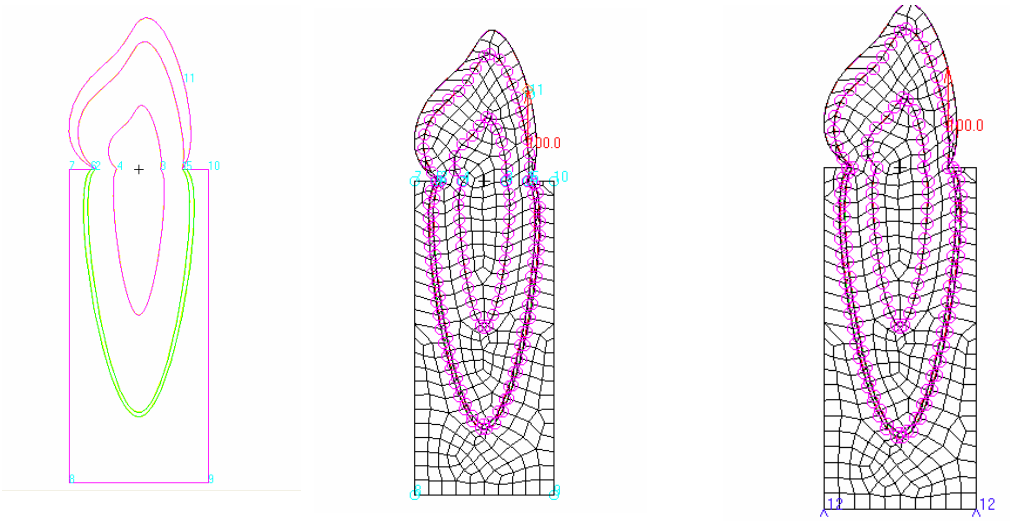

(a) (b) (c)

Figure 3. 16. Defining (a) reference points; (b) concentrated load; (c) boundary conditions for FEA model of madibular first premolar.

3. Result display

Figures 3. 17(a), (b) illustrate the Von mises stresses in fringe and graph formats. Figure 3. 17(c) illustrates the report file for all types of stresses.

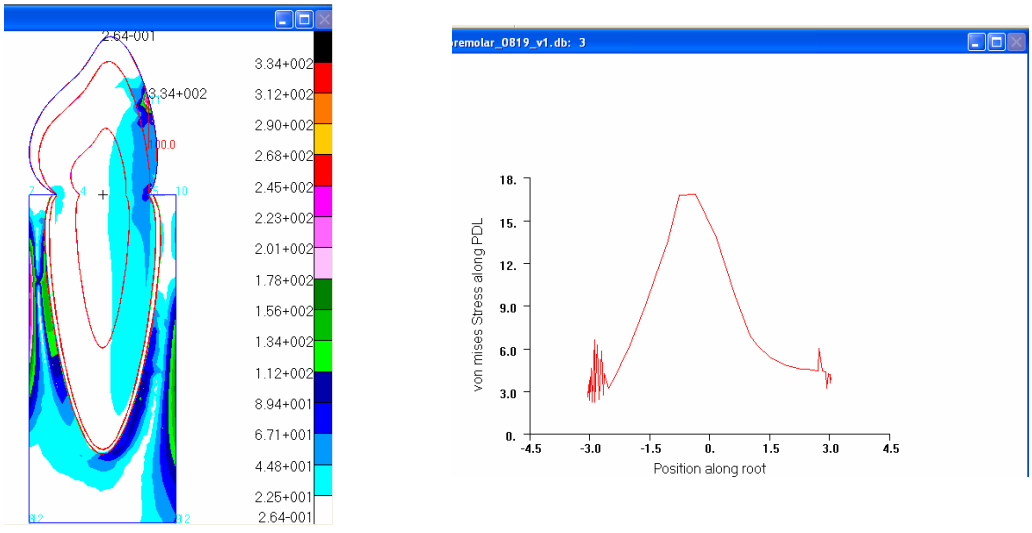

(a) (b)

Figure 3. 17. (a) Fringe of Von mises stress; (b) graph of Von mises stress along PDL.

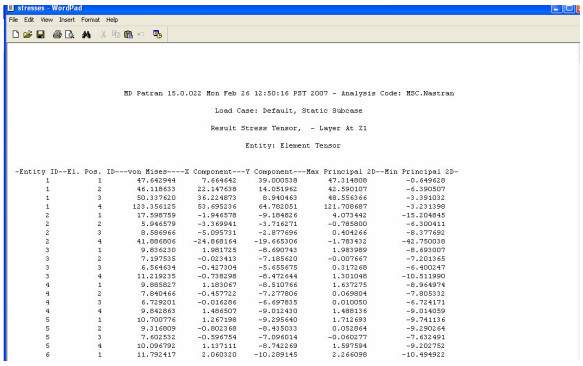

(c)

Figure 3. 17. (continued) (c) report file of stresses for all nodes.

4. Convergence Testing

Table 3. 4 shows the node IDs and coordinates for loads on the tooth models for different levels of mesh refinement. For this example, the original model is refined twice (each time approximately quadrupling the number of elements) to test its convergence (for a total of 3 analyses). Figure 3. 18(a) shows the contents of the “convergence.out” file, which contains the stresses (Von mises, Min principal and Max principal) for the three different levels of mesh refinement at a sequence of geometry points along the sides of the tooth bone where high stresses occur. Figure 3. 18(b) shows the position of the geometry points referenced in the file. For this example, the high stresses occur along the sides of bone, as illustrated in Fig 3. 17(a), thus the geometry points are created for convergence testing along the sides of the bone. The analysis results converge very well in locations of high stress. For example, the “convergence.out” file (Fig 3. 18(a)) shows that for all three cases, there is a Von mises stress concentration at point 4 on the left. This matches the Von mises fringe (Fig 3. 17. (a)) stresses perfectly, which shows that there is a stress concentration at the upper left side bone. At locations of lower stress, e.g. at the

right corner, left corner, etc., local refinement would be necessary if these are deemed to be locations of interest.

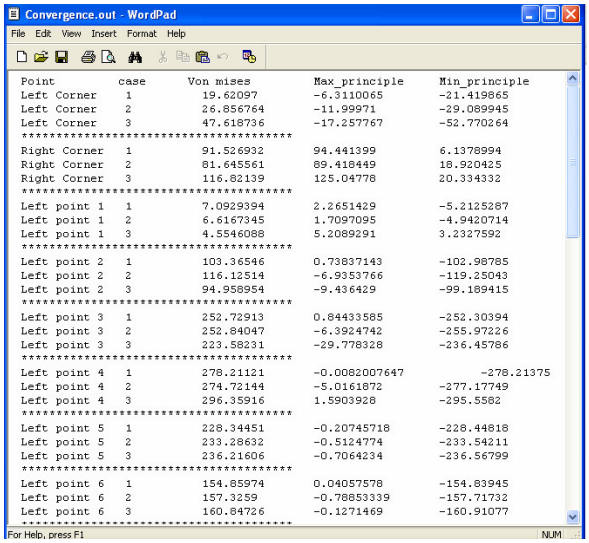

Convergence.out - WordPad

File Edit View Insert Format Help

Point	case	Von mises	Max_principle	Min_principle
Left Corner	1	19.62097	-6.3110065	-21.419865
Left Corner	2	26.856764	-11.99971	-29.089945
Left Corner	3	47.618736	-17.257767	-52.770264
**********				
Right Corner	1	91.526932	94.441399	6.1378994
Right Corner	2	81.645561	89.418449	18.920425
Right Corner	3	116.82139	125.04778	20.334332
**********				
Left point 1	1	7.0929394	2.2651429	-5.2125287
Left point 1	2	6.6167345	1.7097095	-4.9420714
Left point 1	3	4.5546088	5.2089291	3.2327592
**********				
Left point 2	1	103.36546	0.73837143	-102.98785
Left point 2	2	116.12514	-6.9353766	-119.25043
Left point 2	3	94.958954	-9.436429	-99.189415
**********				
Left point 3	1	252.72913	0.84433585	-252.30394
Left point 3	2	252.84047	-6.3924742	-255.97226
Left point 3	3	223.58231	-29.778328	-236.45786
**********				
Left point 4	1	278.21121	-0.0082007647	-278.21375
Left point 4	2	274.72144	-5.0161872	-277.17749
Left point 4	3	296.35916	1.5903928	-295.5582
**********				
Left point 5	1	228.34451	-0.20745718	-228.44818
Left point 5	2	233.28632	-0.5124774	-233.54211
Left point 5	3	236.21606	-0.7064234	-236.56799
**********				
Left point 6	1	154.85974	0.04057578	-154.83945
Left point 6	2	157.3259	-0.78853339	-157.71732
Left point 6	3	160.84726	-0.1271469	-160.91077
**********				

For Help, press F1 NUM

(a)

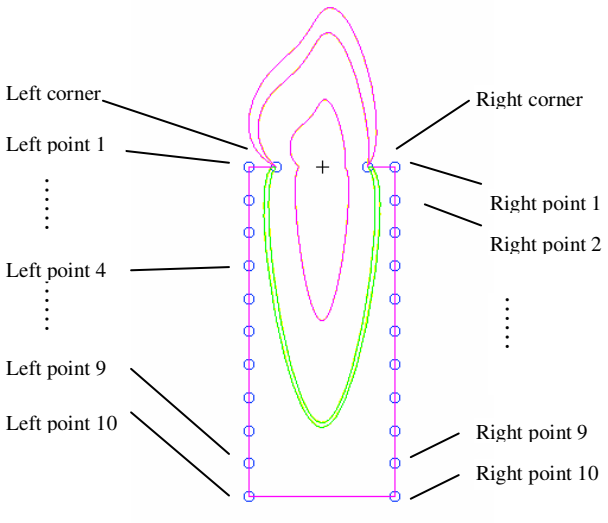

(b)

Figure 3. 18. (a) Convergence output file; (b) geometry points for convergence testing.

Table 3. 4. Stress evaluation locations for each analysis during convergence testing.

Case	Node ID	X_Coord(mm)	Y_Coord (mm)
1	9	2.52	5.28
2	16	2.49	5.39
3	29	2.52	5.25

Occlusal application: This example is for a maxillary second molar under occlusal loads of about 170N distributed along the top surface. A CAD-FEA model in the buccal-lingual direction is generated and analyzed.

1. CAD model creation

The CAD model for a maxillary second molar is shown in Fig 3. 19. The following are the input geometry data:

Tooth type: maxillary second molar

Cross-section direction: labial-lingual

Tooth dimension: default dimensions for maxillary second molar in labial-lingual direction (refer to Table 3. 1.).

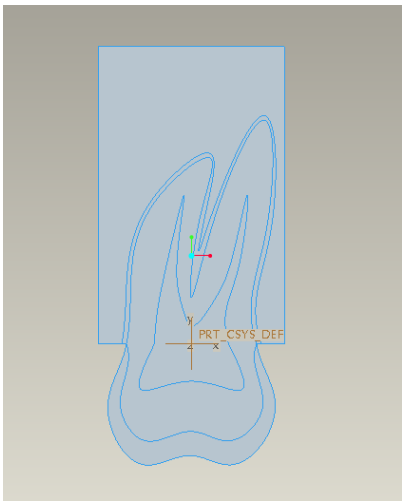

Figure 3. 19. Two-dimensional CAD model for maxillary second molar in labial-lingual direction.

2. FEA model definition

Two reference points are generated for adding distributed loads: point 11 with a space ratio of 0.5 and point 12 with a space ratio of 2, as illustrated in Fig 3. 20(a).

The load type selected is "distributed loads." The distributed load of 2 N/mm (vertical to the curve) is applied to the element edges along the enamel outline between points 11 and 12, as illustrated in Fig 3. 20(b). Then the total loading along the top of tooth is approximately 130N since the distance between point 11 and 12 is about 6.5 mm and the diameter of the tooth crown is about 10 mm.

“Default occlusal constraints” is selected as the boundary condition, as illustrated in Fig 3. 20(c). This fixes the bottom of the tooth bone and prevents movement of the left and right sides of the tooth bone in the horizontal direction.

The material properties used are shown in Table 3.5.

Table 3. 5. Material properties of the tooth model in this example.

	Enamel	Dentine	Pulp	PDL	Bone
Young's modulus (MPa)	85000	19800	2.07	50	13800
Poisson's ratio	0.33	0.31	0.45	0.45	0.3

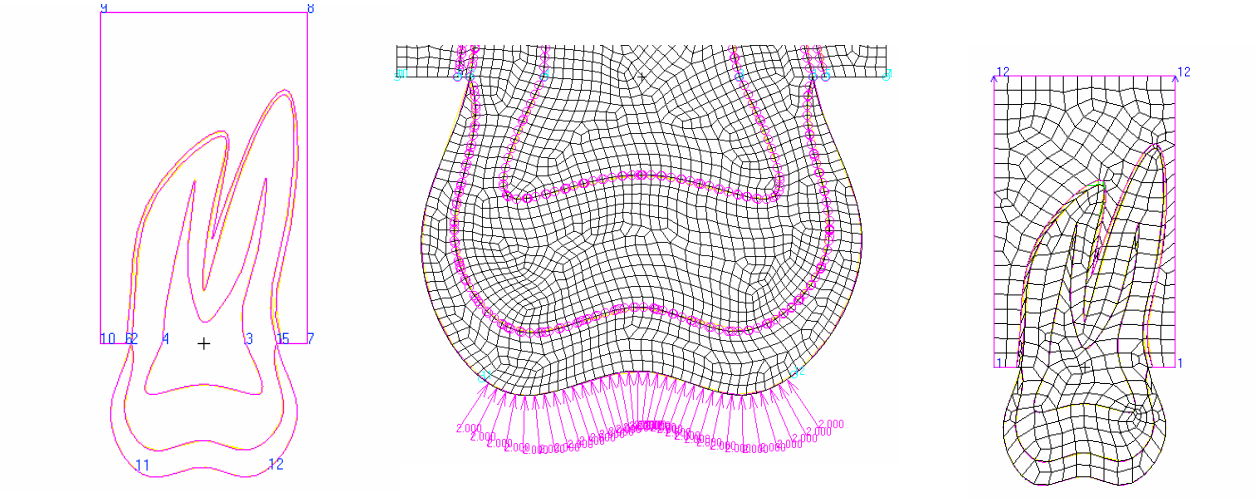

(a) (b) (c)

Figure 3. 20. Defining (a) reference points; (b) distributed loads; (c) boundary conditions for FEA model.

3. Result display

For this example, the minimum principal stress is important since the tooth model is under compression. Figures 3. 21 (a) and (b) show the fringes of Von mises and minimum principal stress distribution, respectively. Figure 3. 21 (c) shows the graph of minimum principal stress distribution along the PDL. Figure 3. 21(d) shows the report file containing all stresses for each node.

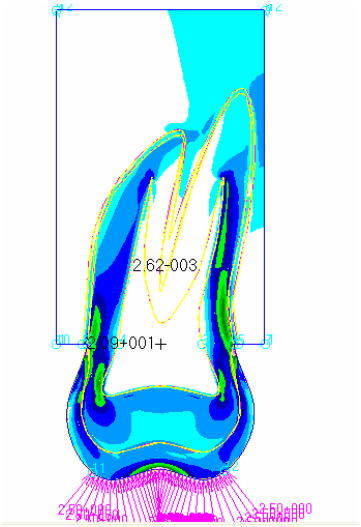

(a)

(b)

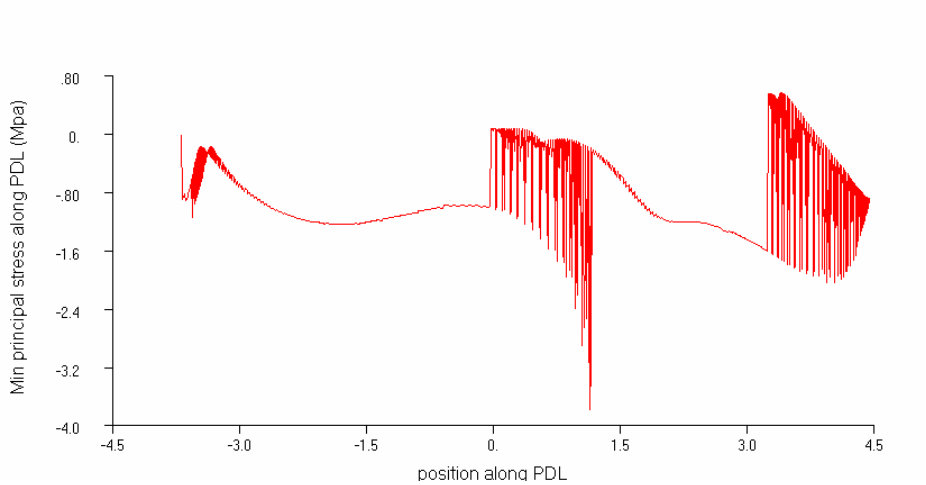

(c)

Figure 3. 21. (a) Fringe of Von mises stress; (b) fringe of minimum principal stress; (c) graph of minimum principal stress along PDL

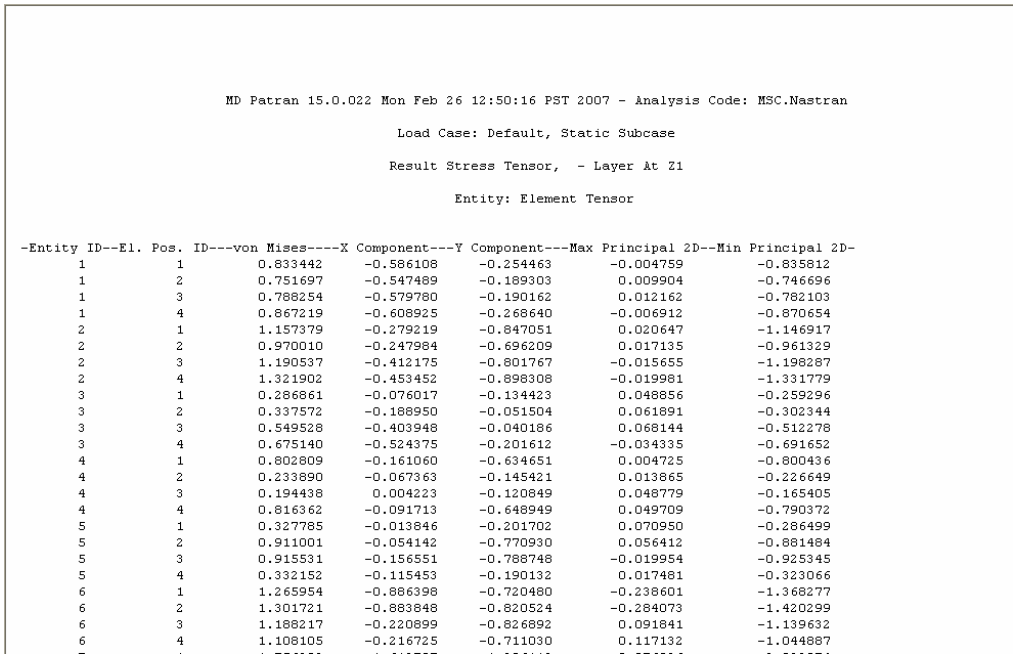

MD Patran 15.0.022 Mon Feb 26 12:50:16 PST 2007 - Analysis Code: MSC.Nastran

Load Case: Default, Static Subcase

Result Stress Tensor, - Layer At Z1

Entity: Element Tensor

-Entity ID-	El. Pos. ID-	--von Mises--	--X Component--	--Y Component--	--Max Principal 2D-	--Min Principal 2D-
1	1	0.833442	-0.586108	-0.254463	-0.004759	-0.835812
1	2	0.751697	-0.547489	-0.189303	0.009904	-0.746696
1	3	0.788254	-0.579780	-0.190162	0.012162	-0.782103
1	4	0.867219	-0.608925	-0.268640	-0.006912	-0.870654
2	1	1.157379	-0.279219	-0.847051	0.020647	-1.146917
2	2	0.970010	-0.247984	-0.696209	0.017135	-0.961329
2	3	1.190537	-0.412175	-0.801767	-0.015655	-1.198287
2	4	1.321902	-0.453452	-0.898308	-0.019981	-1.331779
3	1	0.286861	-0.076017	-0.134423	0.048856	-0.259296
3	2	0.337572	-0.188950	-0.051504	0.061891	-0.302344
3	3	0.549528	-0.403948	-0.040186	0.068144	-0.512278
3	4	0.675140	-0.524375	-0.201612	-0.034335	-0.691652
4	1	0.802809	-0.161060	-0.634651	0.004725	-0.800436
4	2	0.233890	-0.067363	-0.145421	0.013865	-0.226649
4	3	0.194438	0.004223	-0.120849	0.048779	-0.165405
4	4	0.816362	-0.091713	-0.648949	0.049709	-0.790372
5	1	0.327785	-0.013846	-0.201702	0.070950	-0.286499
5	2	0.911001	-0.054142	-0.770930	0.056412	-0.881484
5	3	0.915531	-0.156551	-0.788748	-0.019954	-0.925345
5	4	0.332152	-0.115453	-0.190132	0.017481	-0.323066
6	1	1.265954	-0.886398	-0.720480	-0.238601	-1.368277
6	2	1.301721	-0.883848	-0.820524	-0.284073	-1.420299
6	3	1.188217	-0.220899	-0.826892	0.091841	-1.139632
6	4	1.108105	-0.216725	-0.711030	0.117132	-1.044887

(d)

Figure 3. 21. (continued) (d) report file of stresses for all nodes.

4. Convergence testing

Table 3. 6 shows the values for the distributed loads applied to the tooth model cross-sections for different levels of mesh refinement. For this example, the original model is refined three times to test its convergence (for a total of 4 analyses—each time approximately quadrupling the number of elements). Figure 3. 22 (a) shows the contents of the "convergence.out" file, which contains the stresses (Von mises, maximum principal and minimum principal) for four levels of mesh refinement at geometry points along the outline of enamel where high stresses occur, as illustrated in Figs 3. 21 (a), (b). Figure 3. 22 (b) shows the positions of geometry points 1-13 referenced in the file "convergence.out." The "convergence.out" file (Fig 3. 22 (a)) shows that stress

concentrations are consistently *located* around points 1, 7 and 13 although their *values* do not converge very well at these points. The stresses converge well at points 3-6 and 8-10. These results suggest that local mesh refinement is required around the corner of the enamel (points 1, 2 , 12, and 13); however, it is reasonable that the stresses don't converge well at point 7 since point 7 is located at the center of the distributed loads where the load distribution changes a bit for different mesh refinement levels. The file also shows that the stress values at point 7 are getting smaller and smaller because during mesh refinement, the size of the element edges is getting smaller and smaller causing the loads to be distributed more and more evenly along the outline curve. Generally, the contents of the convergence file match the stress fringes shown in Figs 3. 21(a), (b).

Table 3. 6. Load values in cross-section for each analysis from convergence tests.

Case	Total loads (N)
1	17.23
2	17.30
3	17.37
4	17.21

Point	case	Von mises	Max_principle	Min_principle
point 1	1	5.1199923	-0.28077596	-5.2531867
point 1	2	7.4579864	-0.1820787	-7.5383515
point 1	3	9.4102268	-0.18548903	-9.4794598
point 1	4	7.8220272	-0.22571081	-7.9098363
point 2	1	5.203383	1.1833323	-4.3054304
point 2	2	6.8012571	6.4890876	-0.58037293
point 2	3	5.8577137	3.1991012	-2.6689017
point 2	4	5.4232016	2.2789106	-3.1052921
point 3	1	2.700423	1.1869532	-1.6342255
point 3	2	2.2190459	0.19904038	-2.0298488
point 3	3	2.2160842	0.56791383	-1.7201198
point 3	4	2.1278138	0.43172461	-1.7940335
point 4	1	0.9803502	0.62477171	-0.50512969
point 4	2	2.8678415	0.18050535	-2.7722738
point 4	3	2.6471453	0.14171557	-2.5729527
point 4	4	2.6021776	0.12292154	-2.5378404
point 5	1	2.8650875	-0.38892642	-3.0396833
point 5	2	3.2399755	-1.5187055	-3.669836
point 5	3	3.3630419	-1.3276303	-3.7348354
point 5	4	3.4006791	-1.1993051	-3.7412827
point 6	1	5.3673725	-1.9985924	-6.0799365
point 6	2	5.2654133	-2.0561759	-5.9761276
point 6	3	5.7238407	-2.2435689	-6.5002861
point 6	4	5.5681787	-2.2203951	-6.33182
point 7	1	10.781201	-2.9797058	-11.95645
point 7	2	12.213496	-2.7883203	-13.366165
point 7	3	10.134243	-3.0287299	-11.254292
point 7	4	9.7635927	-3.0445638	-10.872778
point 8	1	5.642529	-1.7657886	-6.31425
point 8	2	5.3430047	-1.9674491	-6.0463758
point 8	3	6.0142393	-2.164247	-6.793467
point 8	4	5.8574996	-2.1899505	-6.6331048
point 9	1	3.6222672	-1.031072	-4.0260186
point 9	2	4.0213757	-1.4917045	-4.5338078
point 9	3	4.0823822	-1.2805833	-4.4918671
point 9	4	4.1008673	-1.2243176	-4.4971242

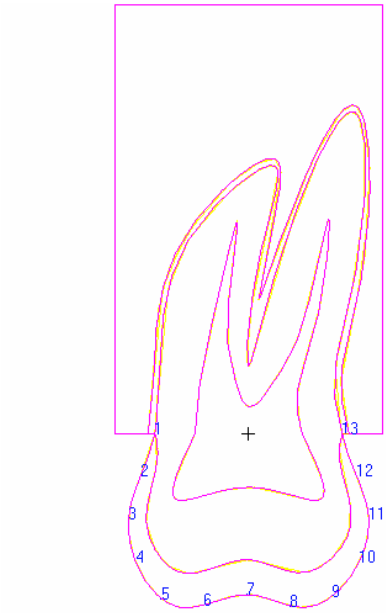

(a) (b)

Figure 3. 22. (a) Convergence output file; (b) geometry points for convergence tests.

Example of geometry optimization: the expert system is applied to the creation and optimization of the geometry for a mandibular labial incisor.

The following are the input geometry data for the CAD model creation:

Tooth type: mandibular labial incisor

Cross-section direction: mesial-distal

Tooth dimension: shown in Fig 3. 23 (a).

The outline curves for enamel will intersect at point (-3.25, 1.55), as shown in Figure 3. 23(b). Figures 3. 23(c) and (d) show the created CAD model without and with

optimization, respectively. Figure 3. 1(b) shows the zoomed-in intersection without optimization, i.e. from Fig 3. 23(c).

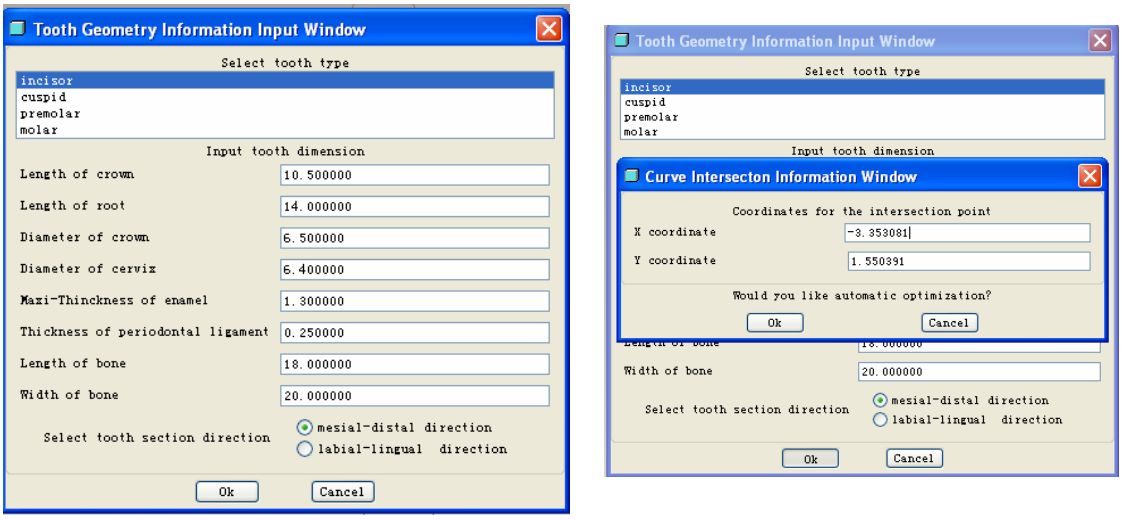

(a) (b)

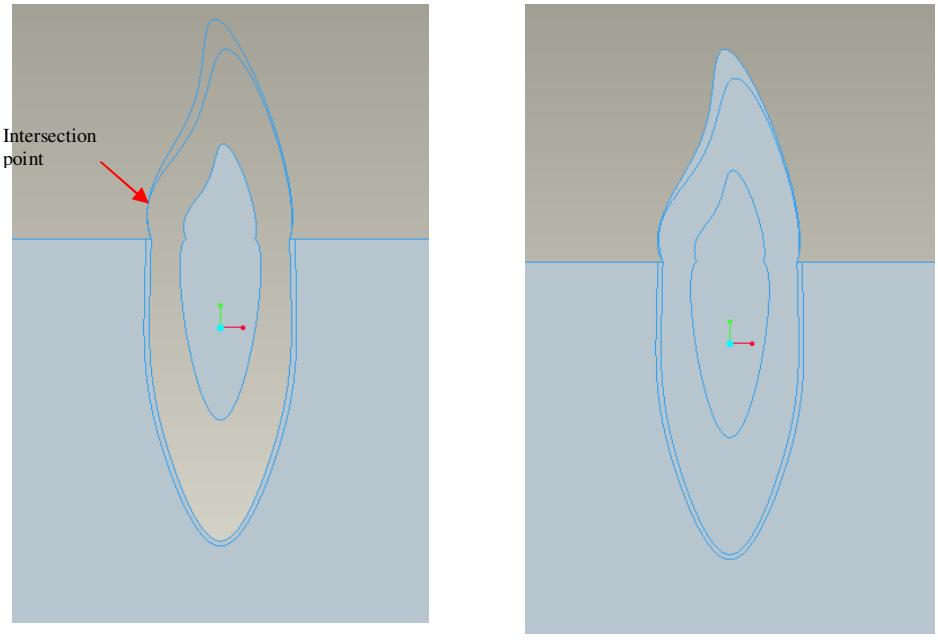

(c) (d)

Figure 3. 23. (a) Geometry information input; (b) curve intersection information output; (c) Tooth geometry without optimization; (d) Tooth geometry with optimization.

CHAPTER IV

CONCLUSIONS

The CAD-FEA model described in Chapter II is a general model that can simulate many situations and be used to perform many different tasks. The shape of any type of tooth can be accurately generated when given enough parameters. Both concentrated loads and distributed loads can be simulated at desired locations. The BC's can be easily defined as needed. The fact that PDL thickness and tooth bone width, etc., can easily be varied demonstrates the usefulness of the general model developed in the present work. Dental practitioners can analyze specific cases and dental researchers can run parametric studies to compare variations when the tooth size, load case, material properties, BC's, etc. are varied. This approach has been further developed with the creation of an expert system, so that the models can be generated automatically through a graphical user interface (GUI).

The expert system:

1. generates CAD-FEA models and performs general tooth stress analysis. By inputting necessary information through GUIs, the geometry of any type of tooth in each cross-section can be generated; both concentrated forces and distributed loads can be defined at any location; the boundary constraints can be defined at any location along any direction; values of material properties can be defined for each tooth part.
2. creates a user friendly environment for researchers and dental practitioners having no background or knowledge of solid mechanics, CAD or FEA. Only geometry

information, loads/BC's and material properties are required. Options such as reference points and default options and values for specific situations are provided for making the process of defining the FEA model as easy as possible. In addition, the system makes decisions for generating the tooth geometry, meshing, and performing the stress analysis automatically. For example, the CAD geometry is optimized and the mesh size is decided automatically; several types of resulting stresses can be displayed in different forms and convergence testing can be performed with results easily accessible for the user to analyze and compare outcomes.

3. speeds up the CAD and FEA simulation process. The time-consuming process of geometry generation and FEA model definition can be completed in minutes by inputting information through GUIs and clicking various selection menus.

4. makes it easy to repeat the CAD and FEA process so that parametric studies become feasible. That is, the values of one or several parameters such as material properties, dimensions, or loads/BC's can be easily changed and then results can be observed as to how these factors affect stress distributions.

Possible future work:

1. Include more default options and decisions for the user. For example, when users input the information for loading conditions, the system can decide which cross-section to create and what BC's to add.

2. Add loads and BC's more easily: automatically find the closest nodes to the reference points and then add the force to the nodes; automatically find the free edges of the elements between two reference points and then add the distributed loads.

3. Automatically locate the high stresses for convergence testing and perform local mesh refinement. The present system requires users to observe the stress concentrations in stress fringes and then define the locations for convergence testing. The present system cannot yet perform local mesh refinement automatically.

4. Develop 3D tooth model geometries for expert CAD-FEA analysis. The 2D CAD-FEA model is only useful for solving problems which can be taken as 2D plane strain. For other problems a 3D CAD-FEA model is needed. No new theory is necessary for this—only the 3D geometries need to be developed.

5. More accurate CAD geometry for a specific tooth may be generated by using digital information obtaining from tooth image scanning. The current generated CAD geometries are general and approximate since they are based on measurements and shape descriptions from the literature. Specific real teeth can be analyzed with scanning technology where the digital information is used to create discrete points first and then generate a 3D CAD geometry.

6. The program can be further developed for including the design of tooth implants and restorations.

Appendix A

Analytic expressions for the outline curves

The outlines of tooth parts can be represented analytically. Each outline of a tooth part is composed of several spline curves and each spline curve is composed of piece-wise cubic polynomials. The coordinates of the points along the *i*th segment of a spline points are[12]:

$$\begin{aligned}(x, y, z) = & \; pnt\_arr[i] * t1\text{^}2 * (1 + 2 * t0) + \\ & pnt\_arr[i+1] * t0\text{^}2 * (1 + 2 * t1) + \\ & (par\_arr[i+1] - par\_arr[i]) * t0 * t1 * \\ & (\tan\_arr[i] * t1 - \tan\_arr[i+1] * t0)\end{aligned} \tag{A1}$$

The parameters are:

$$\begin{aligned}& par\_arr[i] -- \text{the parameter of the first spline point on the } i\text{th segment} \\ & \text{par\_arr}[i+1] \text{ - - the parameter of the last spline point on the } i\text{th segment} \\ & \text{tan\_arr}[i] \text{ - - tangent vectors at the first spline point on the } i\text{th segment} \\ & \text{tan\_arr}[i+1] \text{ - - tangent vectors at the last spline point on the } i\text{th segment} \\ & \text{pnt\_arr[i] - - the interpolant points at the first spline point on the } i\text{th segment} \\ & \text{pnt\_arr[i+1] - - the interpolant points at the last spline point on the } i\text{th segment}\end{aligned} \tag{A2}$$

t0, t1 are:

$$\begin{aligned}& t0 = (\text{t'-par\_arr[i]})/(\text{par\_arr[i+1]} - \text{par\_arr[i]}) \\ & \text{t1} = (\text{par\_arr[i+1]} - \text{t'})/(\text{par\_arr[i+1]} - \text{par\_arr[i]})\end{aligned} \tag{A3}$$

t' is located in the ith spline segment:

$$par\_arr[i] < t' < par\_arr[i+1] \tag{A4}$$

[12] Refer to Pro/Engineer Wildfire 3.0, Pro/Toolkit User's Guide.

Appendix B

Root-finding formula for cubic functions[13]

Root-finding formula based on Cardano's method.

If we have

$$f(x) = ax^3 + bx^2 + cx + d$$
$$with\ a,b,c,d \in R\ and\ a \neq 0, let$$
$$q = \frac{3ac - b^2}{9a^2} \tag{B1}$$
$$and\ \mathrm{r} = \frac{9\mathrm{abc} - 27\mathrm{a}^2 d - 2b^3}{54a^3},$$

$$let\ \ \Delta = \mathrm{q}^3 + r^2 \tag{B2}$$

$$if\ \Delta \geq 0, \text{define}$$
$$\mathrm{s} = \sqrt[3]{r + \sqrt{\Delta}}, \text{and} \tag{B3}$$
$$\mathrm{t} = \sqrt[3]{r - \sqrt{\Delta}}$$

$$else\ if\ \Delta \leq 0,$$
$$there\ \text{are 3 real roots. we express the complex quantity } \mathrm{r} + \mathrm{i}\sqrt{-\Delta}\ \text{in}$$
polar form :
$$\mathrm{r} + \mathrm{i}\sqrt{-\Delta} = (\rho, \theta) \tag{B4}$$
$$\rho = \sqrt{r^2 - \Delta},$$
$$\theta = \mathrm{acos}(\frac{\mathrm{r}}{\rho}),$$

[13] The solution is based on Cardano's method. Reference: Cardano, Gerolamo(1545). Ars Magna.

define :

$$s = (\sqrt[3]{\rho}, \frac{\theta}{3}),$$

and

$$t = (\sqrt[3]{\rho}, -\frac{\theta}{3}).$$

(B5)

in both cases, the solutions are

$$x_1 = s + t - \frac{b}{3a},$$

$$x_2 = -\frac{1}{2}(s+t) - \frac{b}{3a} + \frac{\sqrt{3}}{2}(s-t)i,$$

$$x_3 = -\frac{1}{2}(s+t) - \frac{b}{3a} - \frac{\sqrt{3}}{2}(s-t)i,$$

(B6)

Appendix C

Solution for finding intersection points

A numerical method is used for finding the intersection points between the outline curves of a tooth part. Suppose that there are two spline curves: curve1 and curve2. Both curves start from point A, where y equals to 0. We want to determine if there is an intersection point between the two curves when y varies from 0 to m. The solution is: as illustrated in Figure C. 1, from 0 to m, let the y value increase a small amount at each time step. For each y value, e.g., y=e, calculate the corresponding x1, x2 values for both curves. If x1 is not equal to x2(i.e. the absolute value of "x1-x2" is larger than 10e-6), increase the y value and continue; if x1 equals to x2(i.e. the absolute value of "x1-x2" is smaller than 10e-6), then an intersection point exists at coordinates (x1,m).

Specifically, for our problem, when we suppose a y value on a spline curve, first, we can obtain a cubic equation of t using equation 1. Then we calculate t by solving the equation using root-finding methods; finally, we calculate the x value by repeating using equation1.

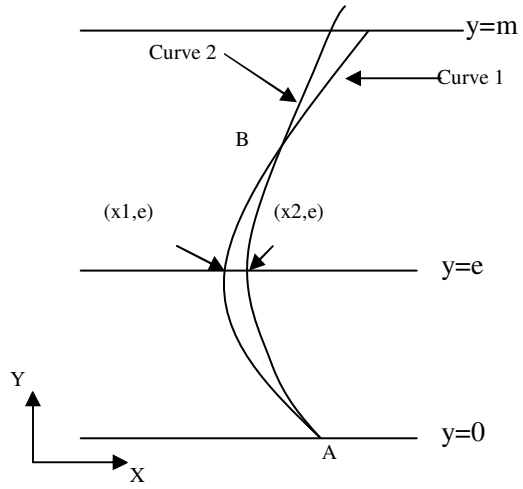

Figure C. 1. Numerical methods for finding intersection points between two curves

Appendix D

Instructions for using the expert system

1. ProToolkit application

   i. Save the application files to C:\HT\Tooth

   ii. Set ProE start in directory: 1) Right click ProEngineer;2) Click "properties" 3) Set the Pro/ Engineer start in as "C:\HT\Tooth", as shown in Fig. D1

   iii. Open ProE, then "Tooth CAD" will appear on the main menu, as shown in Fig 3. 3.

   iv. Click the menu button "Create a template model" under the main menu button "Tooth CAD", and then a template model with datum planes and axes will be generated, as shown in Fig. D2.

   v. Click the menu button "create a tooth model" under the main menu button "Tooth CAD", and then a tooth geometry information input window will appear, as shown in Fig 3. 4(a). Choose the tooth type (incisor, premolar or molar), cross-section direction (mesial-distal or labial-lingual), and input the dimensions. Then click "ok".

   vi. A curve intersection information window will appear if the generated geometry is unreasonable, as shown in Figure 3. 4(b). Click "ok" for automatic geometry optimization.

vii. Then a message will appear prompting the users to input the name for the model and save it as desired filename, as shown in Figure 3. 4(c).

viii. Click the menu button " Export tooth for analysis" under the main menu button "Tooth CAD", a dialogue will appear prompting users to select directory for save the IGES file. Users can select a directory or use the default directory "c:\ht\tooth\parts". Select "open", then an input panel will appear prompting users to input file name for the IGES file. The IGES file will be created in the desired directory when the file name is input.

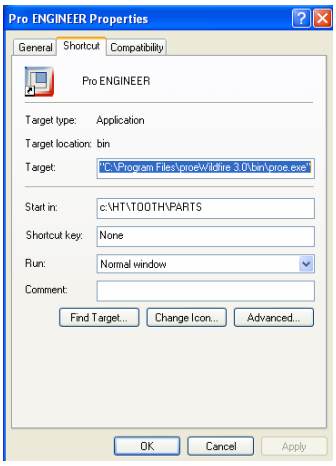

Figure D. 1. Setting the start in directory

2. Patran customization language application

i. Save the application files to C:\Patran\tooth_pcl

ii. Set Patran start in directory: 1) Right click Patran;2) Click "properties" 3) Set the Patran start in as "C:\HT\Tooth", as shown in Fig. D3

iii. Open Patran, then “Tooth FEA” will appear on the main menu, as shown in Figure 3. 6.

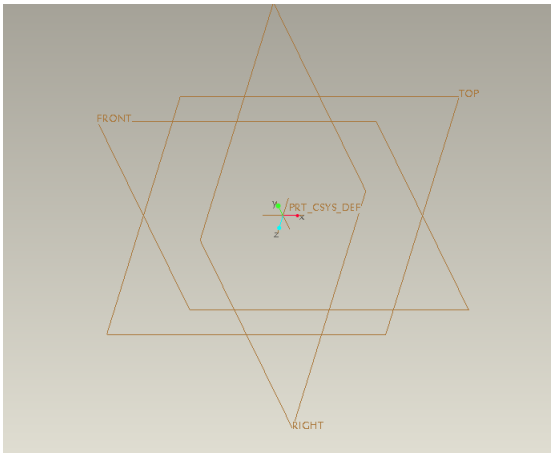

Figure D. 2. A template CAD model with datum plane and axes

Click the menu buttons from “step1- Import Geometry” to “step 10 – Test Convergence” in turn and refer to “graphic user interface” section in Chapter III to perform FEA analysis step by step.

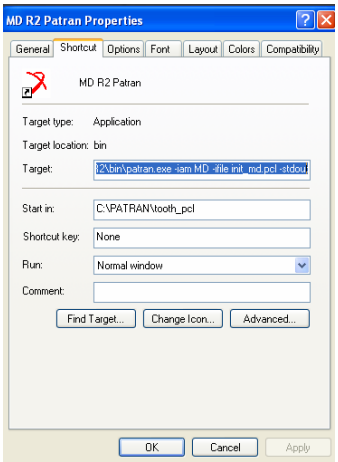

Figure D. 3. Setting Patran start in directory

Appendix E

Contents of the codes packages

	Main Files	Main Functions in the Files	Function Description
CAD	Toolkit.c	user_initialize()	Create main menu and buttons
		toolkit_issue_new()	generate a template part
	Tooth_CAD.c	ProDemoSketchedCurveCreate ()	Create an outline curves for a tooth part
	Matrix.c (PTC provided)	ProUtilPointTrans()	Transform a 2d point to a 3d point
	Ug3DSection.c	UserSectionBuild()	Create 3D section for each outline curve
	List.c	UserUIListImplement()	Create GUIs for tooth geometry information input
		Tooth_classify()	Classify the tooth types
		Inputpanel_DoubuleSet()	Set default tooth dimensions from input panel
		Inputpanel_DoubuleGet()	Get the tooth dimensions from input panel
		SectionDirectionAcitive()	get the selected tooth direction
		list_selecteditemnameActive ()	get the selected tooth type
		list_OKAction()	Action function for the "OK" button
	DefaultSection.c	PremolarDistalEnamel()etc.	Generate spline curves for each tooth part
	SurfaceCreate.c	FillSurface()	Visit the curve feature for surface creation
		intersection_DoubuleSet	Set the coordinates of the intersection points to GUIs
		t_Solution	Calculate the t value for a given y value
		EnamelShapeCheck()	Check if the intersection points exist
		SplineDataObtain()	Retrieve the data of spline curve
		ProSurfaceFeatureCreate()	Create surface feature for each tooth part
	UgInterfaceExport.c	UserIGESGeomflagsExport()	Export the current model to IGES
	Filesaveas.c (PTC provided)	FileSaveAs ()	Save the tooth model with desired name
FEA	IMPORT_TOOTH.pcl	IGES_IMPORT()	Import the IGES file to Patran
	tooth_Interp_ui.cpp	Interpolate_ui	Generate GUI for inputting the information of reference point
	Interp_pnt.pcl	Interp_pnt()	Create the reference points
	MESH_TOOTH.PCL	MESH()	Generate mesh for tooth geometry
	apply_load_to_selected_ nodes.pcl	apply_load_to_selected_nodes( )	Apply load to selected nodes

	distribute_load_to_selected_elements.pcl	distribute_load()	Apply distributed loads to element edges
	apply_boundary_to_selected_edges.pcl	bound_to_edges()	Apply BCs to curves
	apply_boundary_to_selected_nodes.pcl	apply_bound_to_selected_nodes()	Apply BCs to nodes
	boundary_occlusion.pcl	occlusion_default()	Apply default BCs to occlusion case
	boundary_orthodontic.pcl	orthodontic_default()	Apply default BCs to orthodontic case
	force_form.cpp	Force()	Generate GUI for force creation
	DistribLoad_form.cpp	DistribLoad()	Generate GUI for adding distributed load
	boundary_ui.cpp	boundary_ui()	Generate GUI for adding boundary conditioins
	boundary_node.cpp	NODE_FORM	Generate GUI for adding movement restriction on nodes
	boundary_edge.cpp	EDGE_FORM	Generate GUI for adding movement restriction on Edges
	loads_ui.cpp	loads_ui	Generate GUI for adding loads
	properties_tooth.pcl	properties()	Assign the material properties to tooth parts
	properties_ui.cpp	properties_ui()	Generate GUI for adding loads
	enamel_properties.cpp	Enamel	Generate GUI for input material properties for enamel
	dentine_properties.cpp	Dentine	Generate GUI for inputting material properties for dentine
	pulp_properties.cpp	pulp	Generate GUI for inputting material properties for pulp
	PDL_properties.cpp	PDL	Generate GUI for inputting material properties for PDL
	bone_properties.cpp	BONE	Generate GUI for inputting material properties for bone
	tooth_analysis.pcl	Analysis	Analyze the FE model
	tooth_analysis_ui.cpp	analysis_ui	Generate GUI for tooth model analysis
	tooth_read.pcl	Read	Read the results from Nastran to Patran
	select_file.cpp	select_file	Generate GUI for selecting file from desired path
	import_ui.cpp	import_ui	Generate GUI for importing tooth geometry
	Tooth_ResultDisplay_ui.cpp	Tooth_ResultDisplay_ui	Generate GUI for displaying results
	Stress_ui.cpp	Stress_ui	Generate GUI for displaying results of stresses
	Fringe.pcl	Fringe()	Show stresses in fringe format
	Graph.pcl	Graph()	Show stresses in graph format
	Report.pcl	report()	Show stresses in report format

	CONVERGENCE_UI.CPP	Convergence_ui	Generate GUI for convergence test
	MESH_REFINE.PCL	RefineMesh()	Generate mesh
	result_nodes_maxprin2.pcl	Result_nodes_maxprin2()	Retrieve results from database
		Result_convergence	Perform convergence test
	TRAINING.PCL	Training()	Generate “tooth FEA” menu

Appendix F

Log files

The output file are as follows:

a. Spline_curve_3D.txt – retrieved data information for spline curves

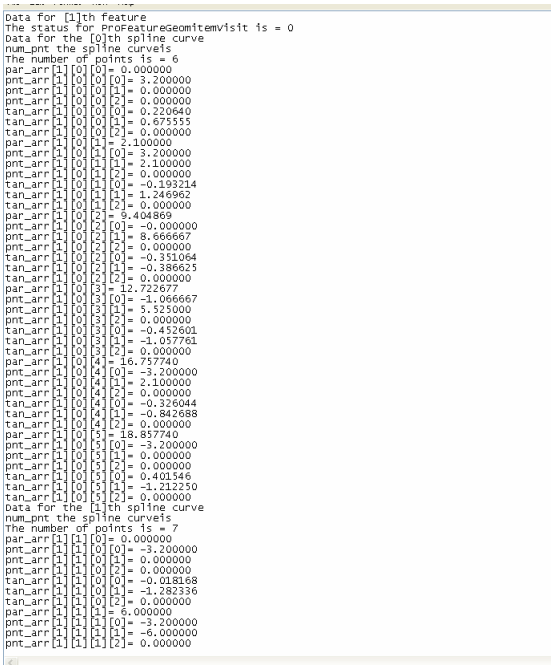

```
Data for [1]th feature
The status for ProFeatureGeomitemVisit is = 0
Data for the [0]th spline curve
num_pnt the spline curveis
The number of points is = 6
par_arr[1][0][0]= 0.000000
pnt_arr[1][0][0][0]= 3.200000
pnt_arr[1][0][0][1]= 0.000000
pnt_arr[1][0][0][2]= 0.000000
tan_arr[1][0][0][0]= 0.220640
tan_arr[1][0][0][1]= 0.675555
tan_arr[1][0][0][2]= 0.000000
par_arr[1][0][1]= 2.100000
pnt_arr[1][0][1][0]= 3.200000
pnt_arr[1][0][1][1]= 2.100000
pnt_arr[1][0][1][2]= 0.000000
tan_arr[1][0][1][0]= -0.193214
tan_arr[1][0][1][1]= 1.246962
tan_arr[1][0][1][2]= 0.000000
par_arr[1][0][2]= 9.404869
pnt_arr[1][0][2][0]= -0.000000
pnt_arr[1][0][2][1]= 8.666667
pnt_arr[1][0][2][2]= 0.000000
tan_arr[1][0][2][0]= -0.351064
tan_arr[1][0][2][1]= -0.386625
tan_arr[1][0][2][2]= 0.000000
par_arr[1][0][3]= 12.722677
pnt_arr[1][0][3][0]= -1.066667
pnt_arr[1][0][3][1]= 5.525000
pnt_arr[1][0][3][2]= 0.000000
tan_arr[1][0][3][0]= -0.452601
tan_arr[1][0][3][1]= -1.057761
tan_arr[1][0][3][2]= 0.000000
par_arr[1][0][4]= 16.757740
pnt_arr[1][0][4][0]= -3.200000
pnt_arr[1][0][4][1]= 2.100000
pnt_arr[1][0][4][2]= 0.000000
tan_arr[1][0][4][0]= -0.326044
tan_arr[1][0][4][1]= -0.842688
tan_arr[1][0][4][2]= 0.000000
par_arr[1][0][5]= 18.857740
pnt_arr[1][0][5][0]= -3.200000
pnt_arr[1][0][5][1]= 0.000000
pnt_arr[1][0][5][2]= 0.000000
tan_arr[1][0][5][0]= 0.401546
tan_arr[1][0][5][1]= -1.212250
tan_arr[1][0][5][2]= 0.000000
Data for the [1]th spline curve
num_pnt the spline curveis
The number of points is = 7
par_arr[1][1][0]= 0.000000
pnt_arr[1][1][0][0]= -3.200000
pnt_arr[1][1][0][1]= 0.000000
pnt_arr[1][1][0][2]= 0.000000
tan_arr[1][1][0][0]= -0.018168
tan_arr[1][1][0][1]= -1.282336
tan_arr[1][1][0][2]= 0.000000
par_arr[1][1][1]= 6.000000
pnt_arr[1][1][1][0]= -3.200000
pnt_arr[1][1][1][1]= -0.000000
pnt_arr[1][1][1][2]= 0.000000
```

b. shape_check.txt – records for the calculating process for intersection point

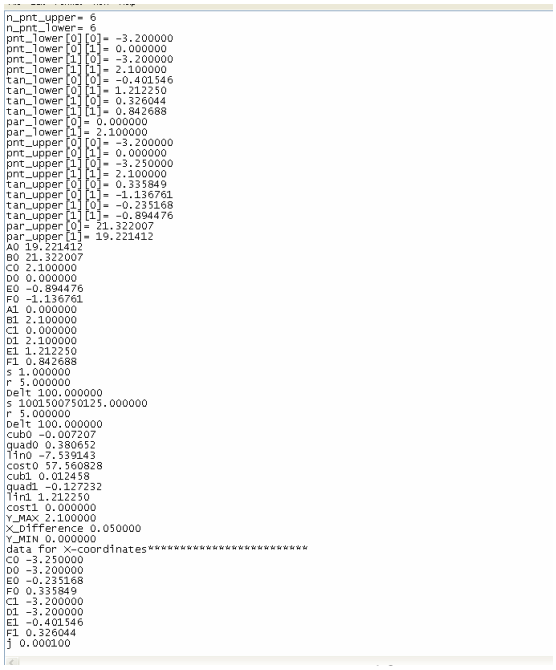

```
n_pnt_upper= 6
n_pnt_lower= 6
pnt_lower[0][0]= -3.200000
pnt_lower[0][1]= 0.000000
pnt_lower[1][0]= -3.200000
pnt_lower[1][1]= 2.100000
tan_lower[0][0]= -0.401546
tan_lower[0][1]= 1.212250
tan_lower[1][0]= 0.326044
tan_lower[1][1]= 0.842688
par_lower[0]= 0.000000
par_lower[1]= 2.100000
pnt_upper[0][0]= -3.200000
pnt_upper[0][1]= 0.000000
pnt_upper[1][0]= -3.250000
pnt_upper[1][1]= 2.100000
tan_upper[0][0]= 0.335849
tan_upper[0][1]= -1.136761
tan_upper[1][0]= -0.235168
tan_upper[1][1]= -0.894476
par_upper[0]= 21.322007
par_upper[1]= 19.221412
A0 19.221412
B0 21.322007
C0 2.100000
D0 0.000000
E0 -0.894476
F0 -1.136761
A1 0.000000
B1 2.100000
C1 0.000000
D1 2.100000
E1 1.212250
F1 0.842688
s 1.000000
r 5.000000
Delt 100.000000
s 1001500750125.000000
r 5.000000
Delt 100.000000
cub0 -0.007207
quad0 0.380652
lin0 -7.539143
cost0 57.560828
cub1 0.012458
quad1 -0.127232
lin1 1.212250
cost1 0.000000
Y_MAX 2.100000
X_Difference 0.050000
Y_MIN 0.000000
data for X-coordinates**************************
C0 -3.250000
D0 -3.200000
E0 -0.235168
F0 0.335849
C1 -3.200000
D1 -3.200000
E1 -0.401546
F1 0.326044
j 0.000100
```

REFERENCES

Arola, D., Galles, L.A., Sarubin, M.F., 2001. A comparison of the mechanical behavior of posterior teeth with amalgam and composite MOD restorations. Journal of Dentistry 29, 63-73.

Ash M.M (1984). Wheeler's atlas of Tooth Form, 5th edn, W.B. Saunders Co., Philadelphia, PA.

Ash M.M (1993). Wheeler's Dental Anatomy, Physiology and Occlusion. W.B. Saunders Co., Philadelphia, PA.

Ausiello, P., Apicella, A., Davidson, C.L., Rengo, S., 2001. 3D-finite element analyses of cusp movements in a human upper premolar, restored with adhesive resin-based composites. Journal of Biomechanics 34, 1269-1277.

Borcic, J., Anic, I., Smojver, I., Catic, A., Miletic, I., Ribaric, S.P., 2005. 3D finite element model and cervical lesion formation in normal occlusion and in malocclusion. Journal of Oral Rehabilitation 32, 504-510.

Chang KH, Magdum S, Khera SC, Goel VK (2003). An advanced approach for computer modeling and prototyping of the human tooth. *Annals of Biomedical Engineering* 31: 621-631.

Chen KZ, Feng XA, Lu QS (2002). Intelligent location-dimensioning of cylindrical surfaces in mechanical parts. *Computer-Aided Design*, 34: 185-194.

Choi JC, Kim BM, Cho HY, Kim C, Kim JH (1998). An integrated CAD system for the blanking of irregular-shaped sheet metal products**.** *J Materials Processing Technology*, 83(1-3): 84-97.

Dejak, B., Mlotkowski, A., Romanowicz, M., 2003. Finite element analysis of stresses in molars during clenching and mastication. Journal of Prosthetic Dentistry 90, 591-597.

Grine FE (2005). Enamel Thickness of Deciduous and Permanent Molars in Modern *Homo sapiens*. American journal of physical anthropology. 126:14–31.

Lanza A, Aversa R, Rengo S, Apicella D, Apicella A (2005). 3D FEA of cemented steel, glass and carbon posts in a maxillary incisor. *Dental Materials* 21: 709-715.

Lee KH, Lee JK, Park NS (1998). Intelligent approach to a CAD system for the layout design of a ship engine room. *Computers & Industrial Engineering,* 34(3): 599-608.

Li Q, Rubin CA (2004). Virtual Prototype Design and Testing – Simplifying the CAD/Analysis Interface, *Proc FISITA 2004 World Automotive Congress*, Barcelona.

Liebowitz J (1995). Expert systems: A short introduction. *Engineering Fracture Mechanics*, 50, 5-6: 601-607.

Lin CL, Chang CH, Cheng CS, Wang CH, Lee HE (1999). Automatic finite element mesh generation for maxillary second premolar. *Computer Methods and Programs in Biomedicine* 59: 187-195.

Lin, C.L., Chang, Y.H., Chang, W.J., Cheng, M.H., 2006. Evaluation of a reinforced slot design for CEREC system to restore extensively compromised premolars. Journal of Dentistry 34, 221-229.

Lindhe J, Karring T (1989). The anatomy of the periodontium. In: Lindhe J, Karring J, eds. Textbook of Clinical Perodontology. 2nd ed. Copenhagen: Munksgaard; 19-69.

Magne P (2006). Efficient 3D finite element analysis of dental restorative procedures using micro-CT data. *Dental Materials* 23: 539-548.

Motta A, Pereira L, Cunha A(2006). Finite Element Analysis in 2D and 3D Models for Sound and Restored Teeth. ABAQUS Users' Conference.

Myung S, Han S (2001). Knowledge-based parametric design of mechanical products based on configuration design method. *Expert Systems with Applications*, 21(2): 99-107.

Ochiai, K.T., Ozawa S., Caputo, A.A., Nishimura, R.D., 2003. Photoelastic stress analysis of implant-tooth connected prostheses with segmented and nonsegmented abutments. Journal of *Prosthetic Dentistry* 89, 495-502.

Palamara JE, Palamara D, Messer HH (2002). Strains in the marginal ridge during occlusal loading. *Australian Dental Journal* 47: 218-222.

Romeed, S.A., Fok, S.L., Wilson, N.H., 2004. Finite element analysis of fixed partial denture replacement. Journal of Oral Rehabilitation 31, 1208-1217.

Robinson PA, Swift KG, Raines M, Graham RH, Peckover S, Gill L (2001). An expert system for the determination of stress concentration factors. *Proc Instn Mech, IMechE 2001*, 215(G): 219-228.

Rubin C, Chan W, Hutchinson, V, Jones G (2002). Virtual Design and Testing for Manufacturing - The Solid Model - Finite Element Analysis Interface, *Proceedings of Aerospace - A 2020 Vision: Technological Challenges from Concept to Disposal*, Royal Aeronautical Society, London.

Rubin, C., Krishnamurthy, N., Capilouto, E., Yi, H., 1983. Stress Analysis of the Human Tooth Using a Three-Dimensional Finite Element Model. Journal of Dental Research 62, 82-86.

Rubin, C., Yi, H., Capilouto, E., 1982. Stress Distribution in Restorations, A Three-Dimensional Finite Element Study. *Proceedings of the First Southern Biomedical Engineering Conference*, Shreveport, LA: 318-321.

Schwartz RS, Summitt JB, Robbins JW, Santos JD (1996). Fundamentals of operative dentistry. Chicago: Quintessence.

Song JH, Im YT (1999). Expert system for the process sequence design of a ball stud. *Journal of Materials Processing Technology,* 89-90: 72-78.

Tanaka M, Naito T, Yokota M, Kohno M (2003). Finite element analysis of the possible mechanism of cervical lesion formation by occlusal force. *Journal of Oral Rehabilitation* 30: 60-67.

Toms SR, Eberhardt AW (2003). A nonlinear finite element analysis of the periodontal ligament under orthodontic tooth loading. *American Journal of Orthodontics and Dentofacial Orthopedics* 123: 657-665.

Toparli, M., Aykul, H., Sasaki, S., 2003. Temperature and thermal stress analysis of a crowned maxillary second premolar tooth using three-dimensional finite element method. Journal of Oral Rehabilitation 30, 99-105.

Toparli, M., Sasaki, S., 2003. Finite element analysis of the temperature and thermal stress in a postrestored tooth. Journal of Oral Rehabilitation 30, 921-926.

Topbasi, B., Gunday, M., Bas, M., Turkmen, C., 2001.Two-dimensional photoelastic stress analysis of traumatized incisor. *Brazilian Dental Journal* 12(2), 81-84.

Wang, M.Q., Zhang, M., Zhang, J.H., 2004. Photoelastic study of the effects of occlusal surface morphology on tooth apical stress from vertical bite forces. Journal of Contemporary Dental Practice 5, 74-93.